4.0 SITE HYDROGEOLOGY

This section briefly describes the results of monitoring pressure and temperature in UE-25 ONC#1 and USW NRG4. A more comprehensive presentation of the results of monitoring is presented in Multimedia Environmental Technology, Inc. (1996) and is posted on a monthly basis on the Internet (www.nyecounty.com). The UE-25 ONC#1 borehole was drilled and both UE-25 ONC#1 and USW NRG4 boreholes were instrumented to support the following data collection activities:

1. To monitor the long-term variation of pressure and temperature in hydrogeologic units that may be impacted by the construction of the ESF.

2. To perform vacuum and/or injection pneumatic testing to evaluate the horizontal and, to some extent (unknown), vertical pneumatic conductivity values of the hydrogeologic units packed off by the Westbay Instruments.

3. To sample intervals isolated by packers for environmental isotopes to evaluate the residence time of the gases in the hydrogeologic formations.

Nye County borehole locations were selected primarily to establish baseline conditions before penetration of the repository host rock by the ESF tunnel and to monitor the effects of the mine ventilation system used in the ESF tunnel on the ambient pneumatic and moisture conditions of the unsaturated zone in the vicinity of the north and south ramps of the ESF tunnel. UE-25 ONC#1 is situated southeast of the repository block and is in the path of the future South Ramp of the ESF tunnel (Figure 1-2). It was also strategically located to be along the main trace of the Bow Ridge Fault system and close enough to DOE's C Well Complex (approximately 800 meters) to serve as a monitoring well during aquifer testing. It was drilled by Nye County in late 1994 and early 1995 using dual wall reverse circulation technology to demonstrate an alternative drilling and sampling method to DOE (NWRPO, 1995).

USW NRG4 is located northeast of the repository block (Figure 1-2) and is situated about 1100 m from the North Ramp (NR) portal of the ESF tunnel. It was previously drilled by DOE. The ESF tunnel passed within approximately 15 meters of USW NRG4 in the middle of June 1995. The effects of the tunnel excavation on pneumatic conditions in this instrumented borehole, as well as in UE-25 ONC#1, will be discussed in the following sections.

Nye County instrumented UE-25 ONC#1 and USW NRG4 in early 1995 with Westbay Corporation's MOSDAX MP55 system. The MP-55 is a multilevel monitoring device that consists of an access casing with multiple ports or valves that can be opened to the formation. A multilevel packer system integrated into the access tube serves to isolate access ports and retrievable temperature/pressure measurement probes that connect to these access ports. An above ground data logger is used to monitor the temperature/pressure probes. A complete description of this downhole monitoring system and installation procedures in these boreholes is presented in NWRPO (1995).

Fifteen downhole packers were used to isolate major stratigraphic units, a fault zone, and two isolated zones below the water table in UE-25 ONC#1. Figure 4-1 shows the location of 15 packers and 31 measurement ports in relation to stratigraphic units, the Bow Ridge fault zone, and the water table. MOSDAX temperature/sensor probes were installed in 9 of the 31 measurement ports available. It should be noted that the two bottom-most probes in UE-25 ONC#1 are situated below the water table and are monitoring the piezometric potential.

Seven downhole packers and 7 measurement ports were strategically installed in major stratigraphic units in USW NRG4 as shown in Figure 4-1. MOSDAX temperature/sensor probes were installed in all 7 measurement ports.

The pressure and temperature in UE-25 ONC#1 and USW NRG4 have been monitored since April 1995. Figures 4-2 through 4-13 are graphical representations of the pressure and temperature readings for the months of June

1997, October 1997, and March 1998 for each borehole. Graphs for the time period of April 1997 through May 1998 are presented in the accompanying media package (see Onc1Press&Temp.ppt and Nrg4Press&Temp.ppt). Temperatures reported for all downhole instruments are fairly stable with occasional deviations from the norm. The atmospheric probe (Probe 0) in each borehole records a wide range of daily and seasonal temperature fluctuations typical of a desert environment. Comparison of the temperature data from atmospheric probes in USW NRG4 and UE-25 ONC#1 indicates very consistent atmospheric temperature patterns at the two borehole sites.

Pressure fluctuations with time for UE-25 ONC#1 and USW NRG4 show that pressure responses exhibit trends versus depth that are expected in layered geologic media. That is, there is a general dampening of the magnitude as well as an increasing time-lag in the peaks and valleys of barometric pressure fluctuations as depth increases. The only exception to these trends are data collected from April to August 1995 in UE-25 ONC#1 when the upper portion of the borehole was opened to the atmosphere and in both boreholes after the tunnel penetrated the proposed repository horizon.

Two of the probes in UE-25 ONC#1 (Probes 8 and 9) are below the water table. These probes monitor variation of piezometric level with time.

Comparison of Probe-0 pressure responses at USW NRG4 and UE-25 ONC#1 indicate nearly identical responses over time when corrected for elevation differences.

Nye County has also received data from unsaturated zone boreholes monitored by U. S. Geological Survey's. These data were analyzed and graphed to compare the data collected by the Yucca Mountain Project (U.S. Geological Survey) with those collected by Nye County. These graphs show that, despite the significant difference in the data collection techniques, there is a close agreement between the averages of the data. The slight differences in the trends and magnitudes are

expected due to the position of the boreholes with respect to the natural and man-made boundary conditions.

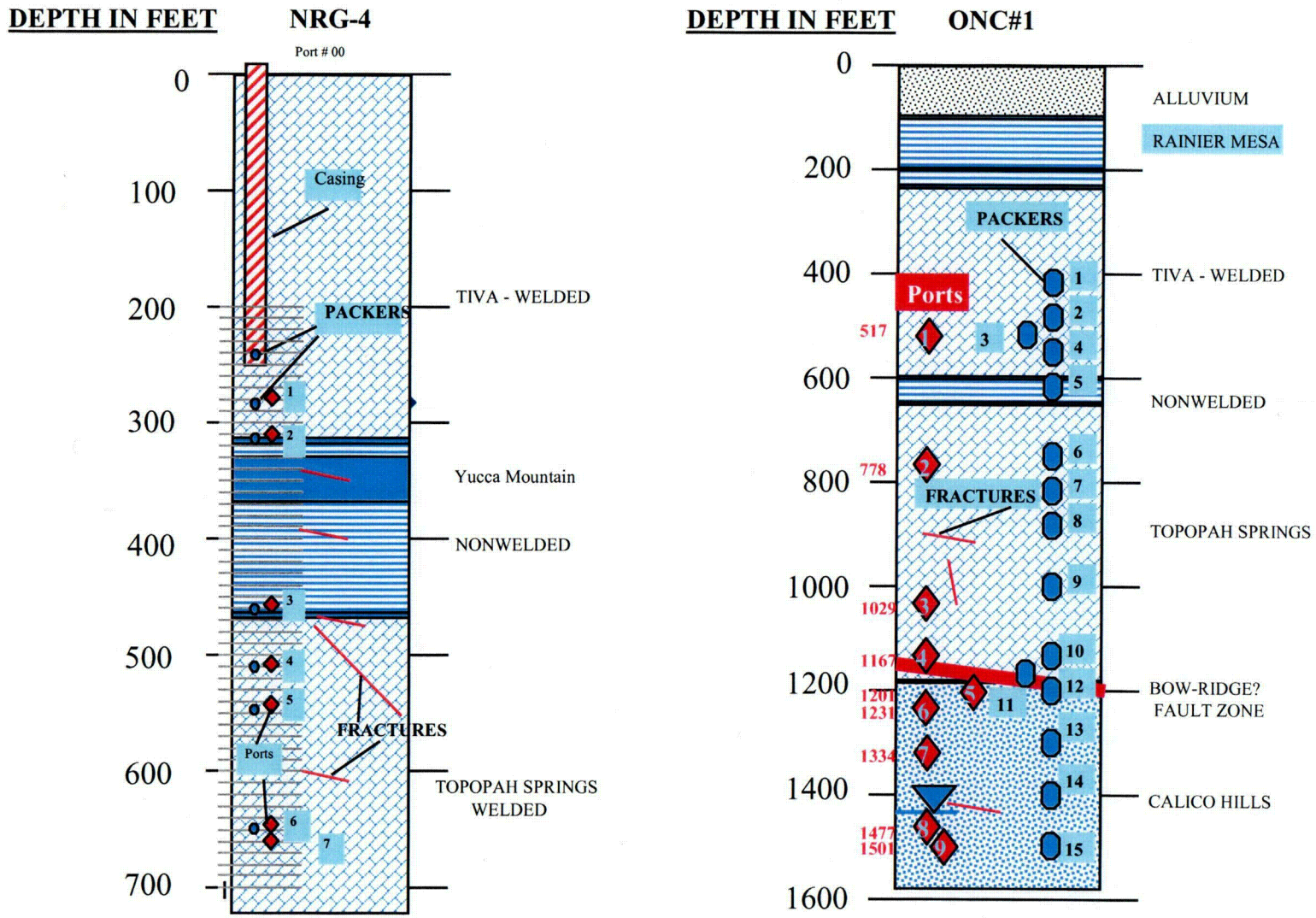

Figure 4-1 Schematic profile of instrumentation setup in UE-25 ONC# 1 and USW NRG-4.

C-01

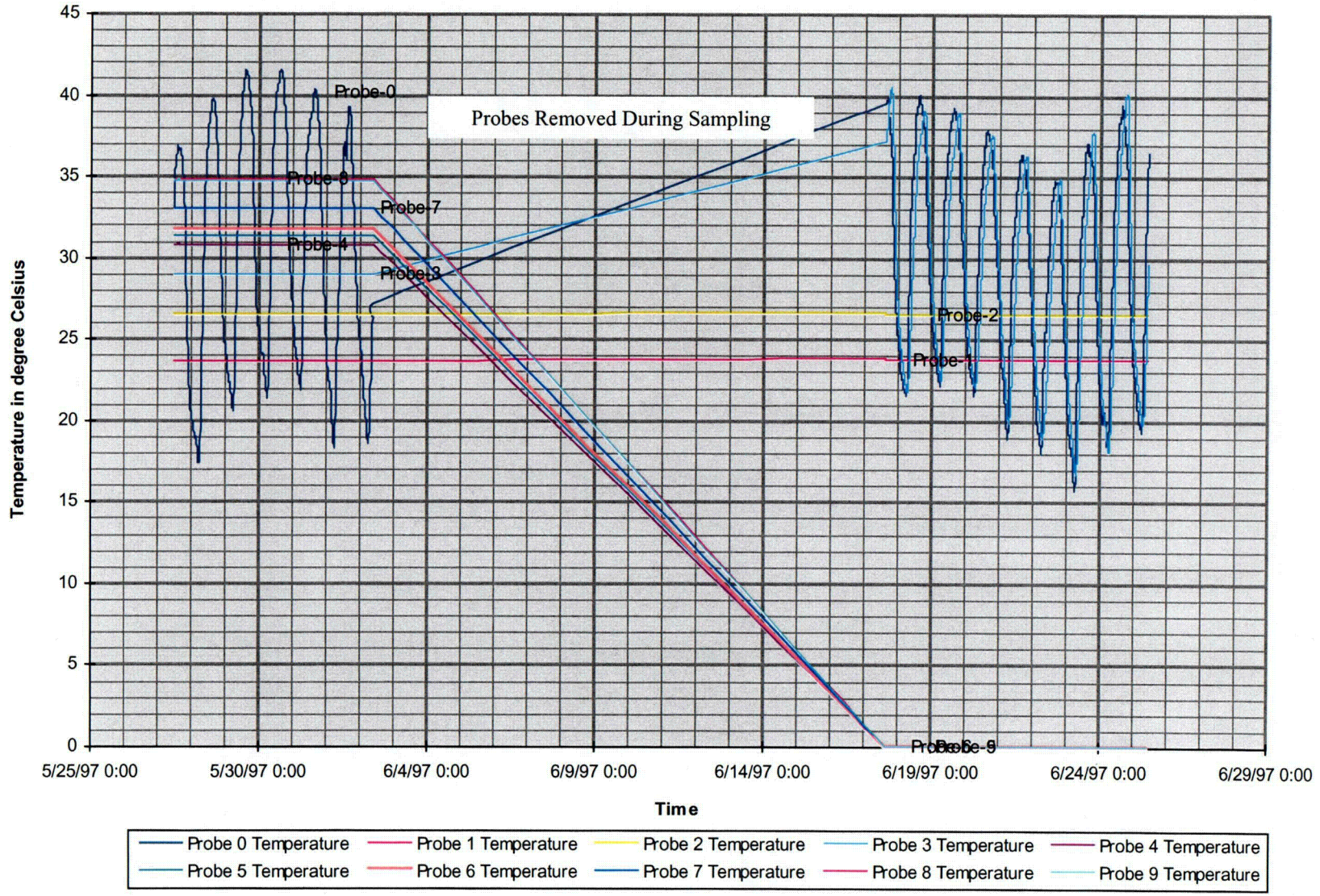

Figure 4-2 **Temperature variation with time in ONC#1 corrected with interpolation calibration, June 1997.**

C-02

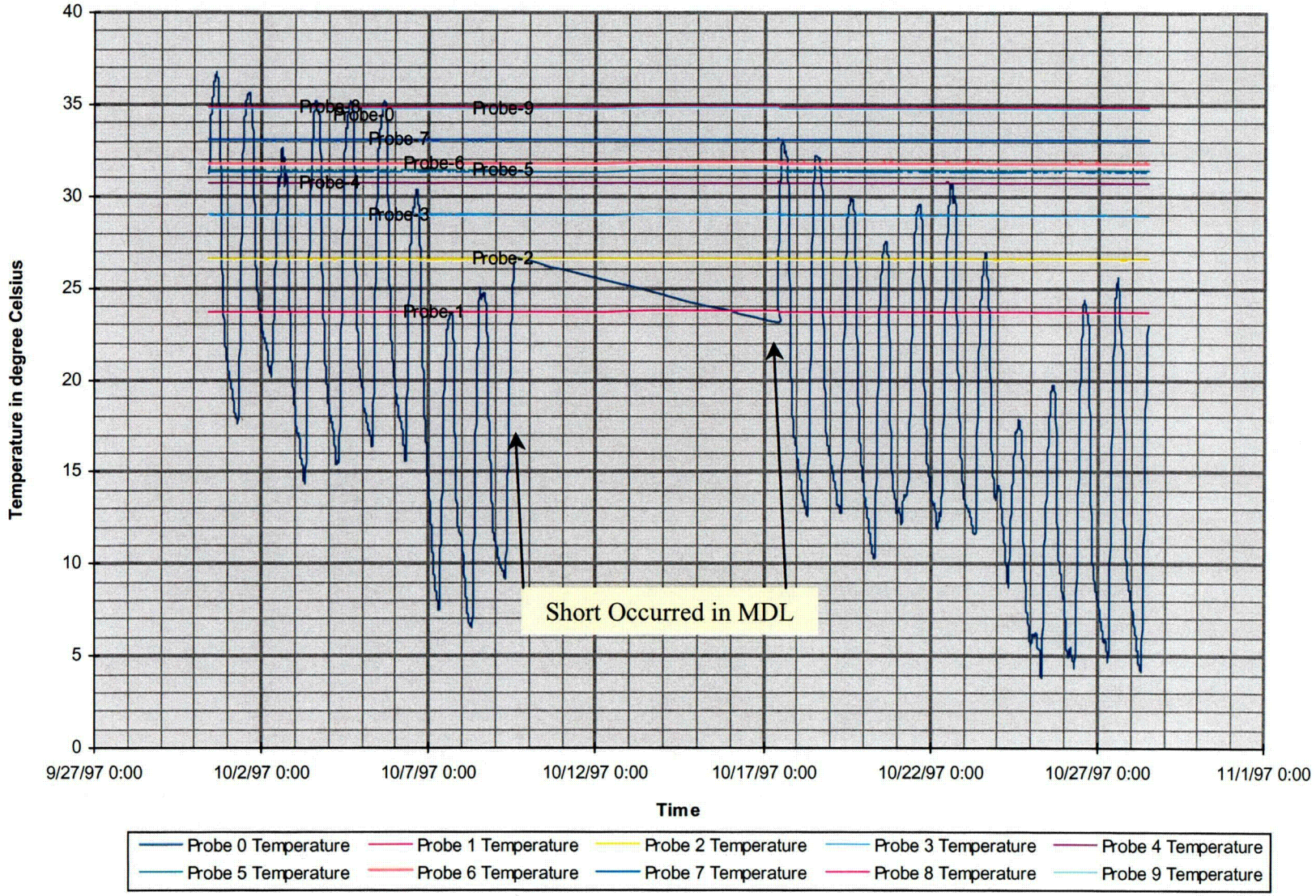

Figure 4-3 Temperature variation with time in ONC#1 corrected with interpolation calibration, October 1997.

C-03

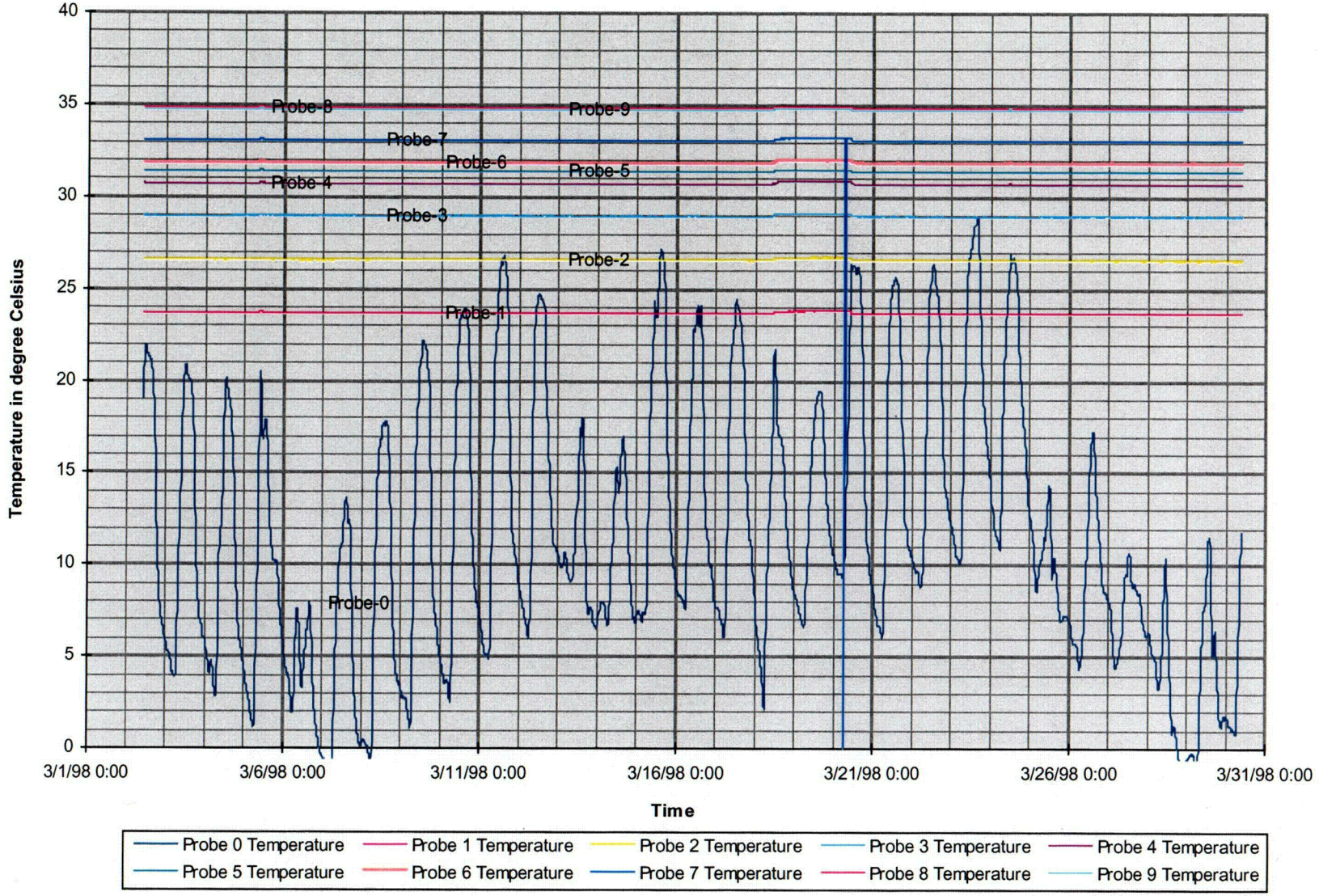

Figure 4-4 **Temperature variation with time in ONC#1 corrected with interpolation calibration, March 1998.**

C-04

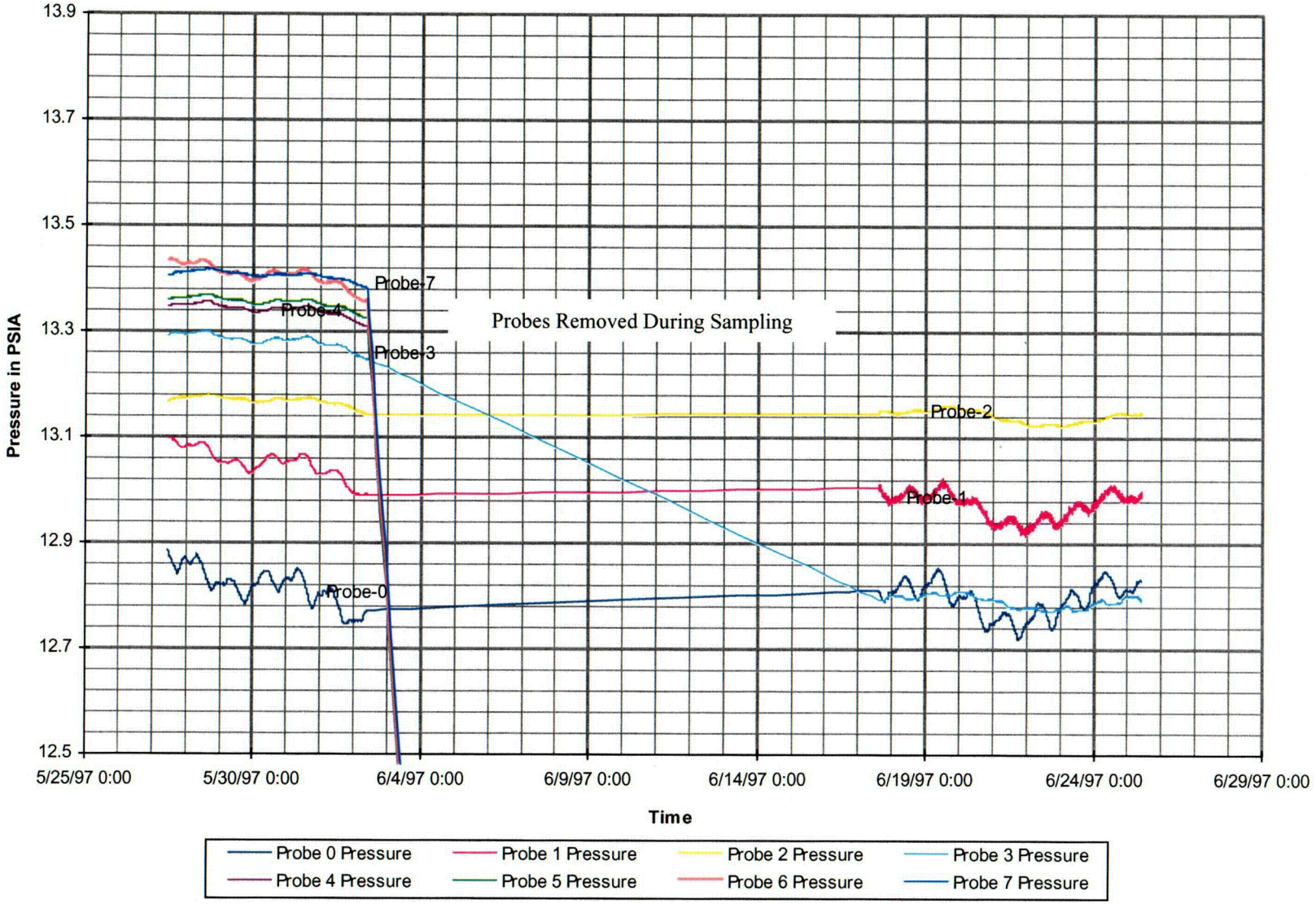

Figure 4-5 Absolute pressure for ONC#1 corrected with interpolation calibration, June 1997.

C-05

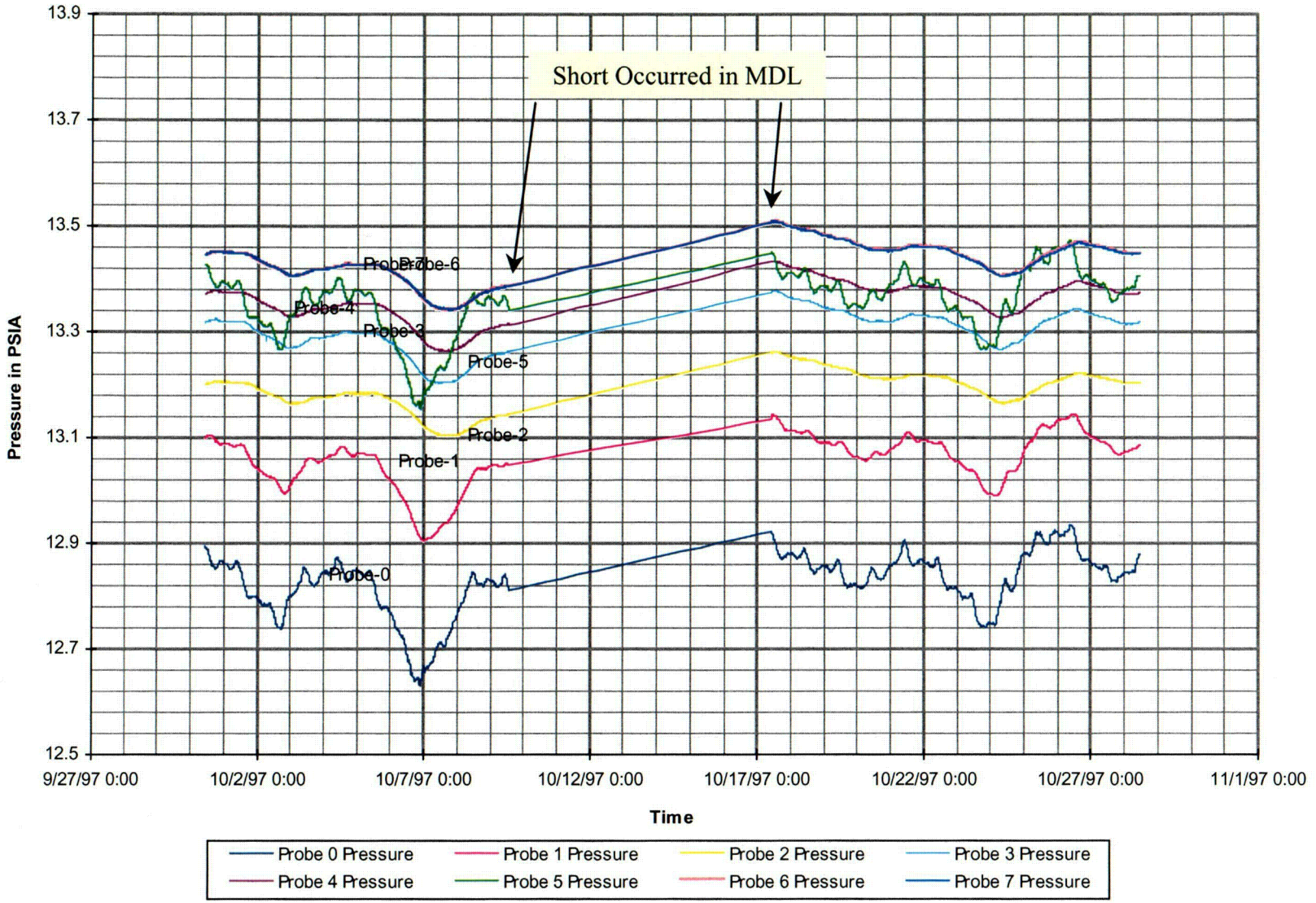

Figure 4-6 **Absolute pressure for ONC#1 corrected with interpolation calibration, October 1997.**

C-06

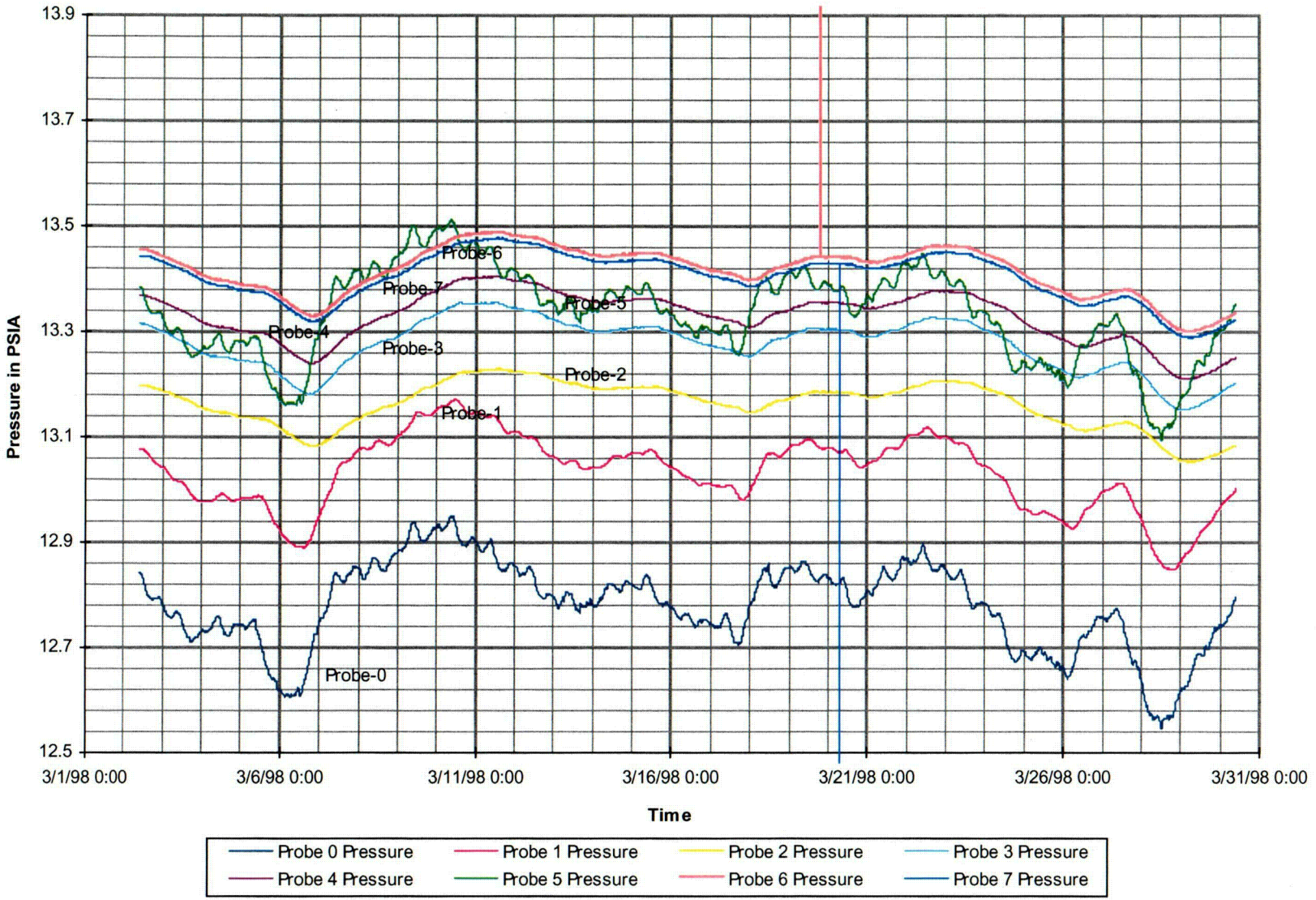

Figure 4-7 **Absolute pressure for ONC#1 corrected with interpolation calibration, March 1998.**

C-07

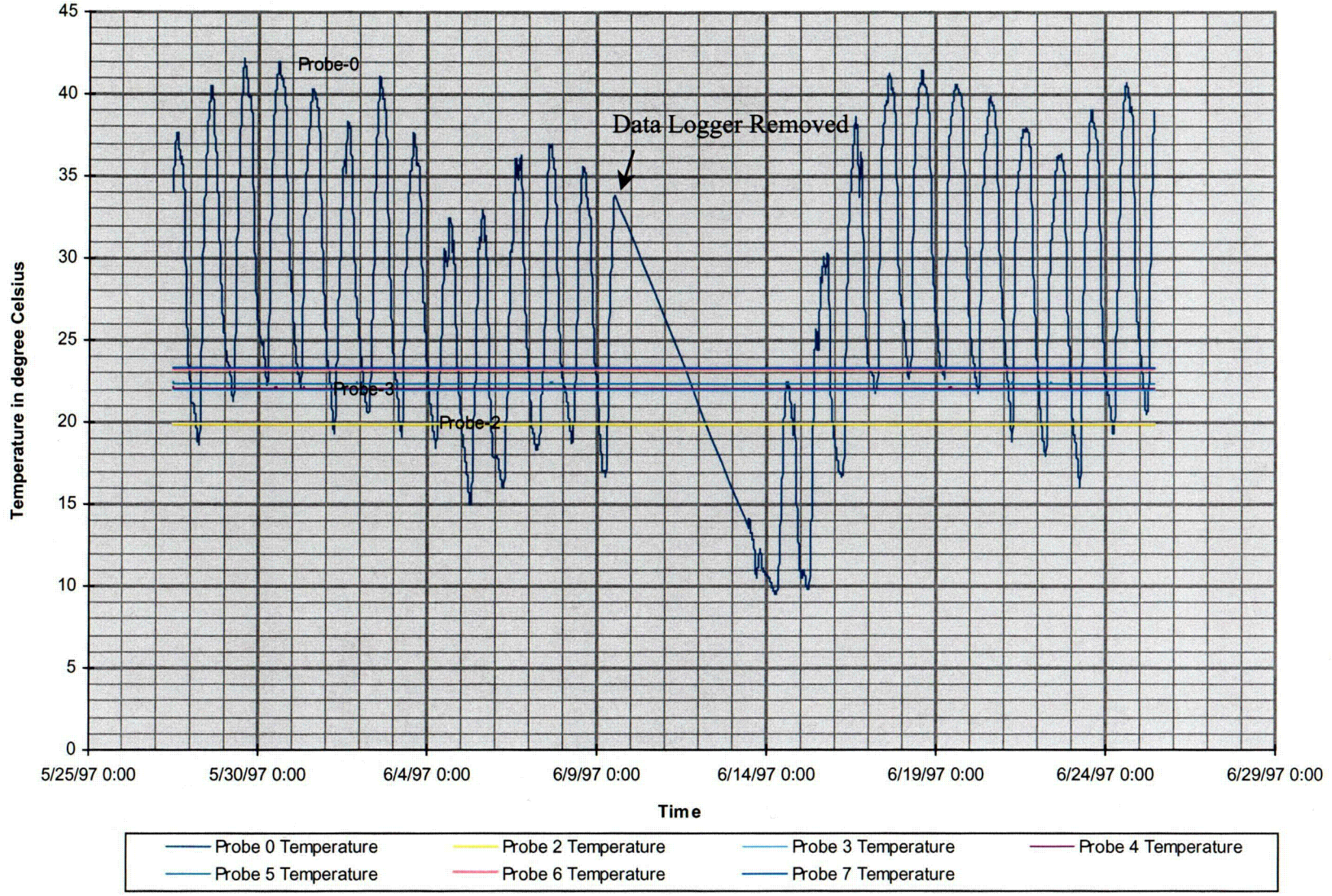

Figure 4-8 Temperature variation with time in NRG-4 corrected with interpolation calibration, June 1997.

C-08

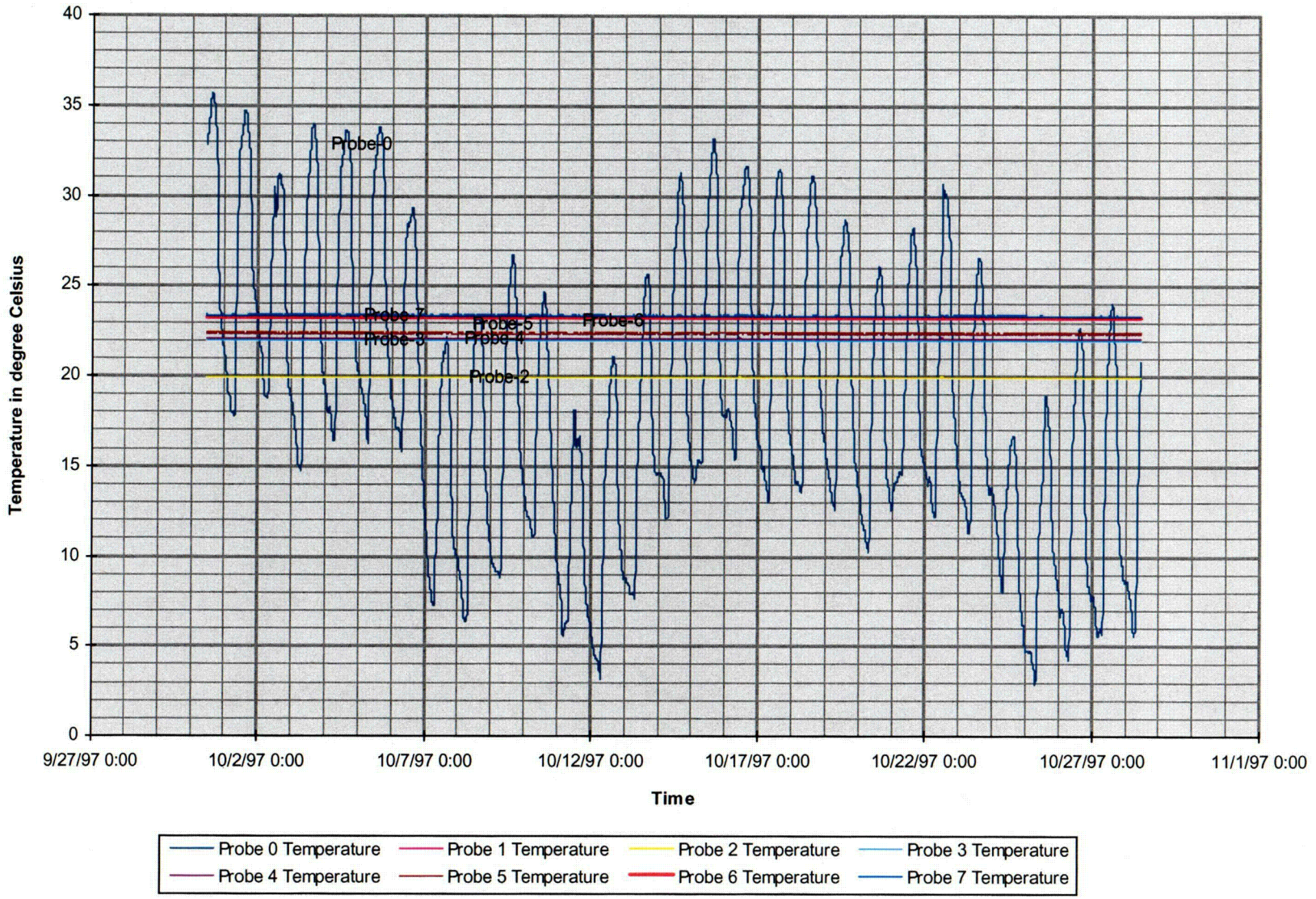

Figure 4-9 **Temperature variations with time in NRG-4, October 1997.**

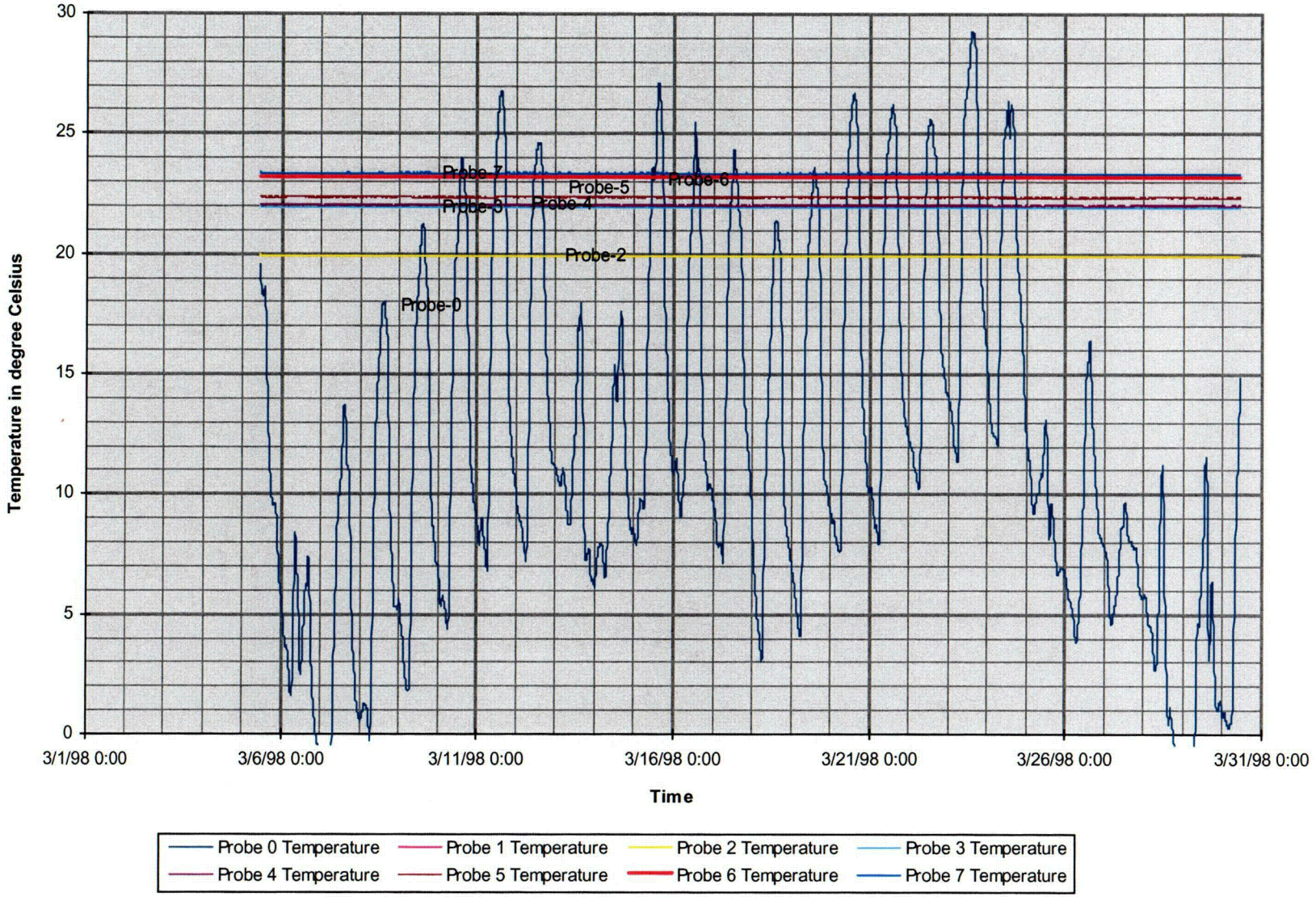

Figure 4-10 Temperature variations with time in NRG-4, March 1998.

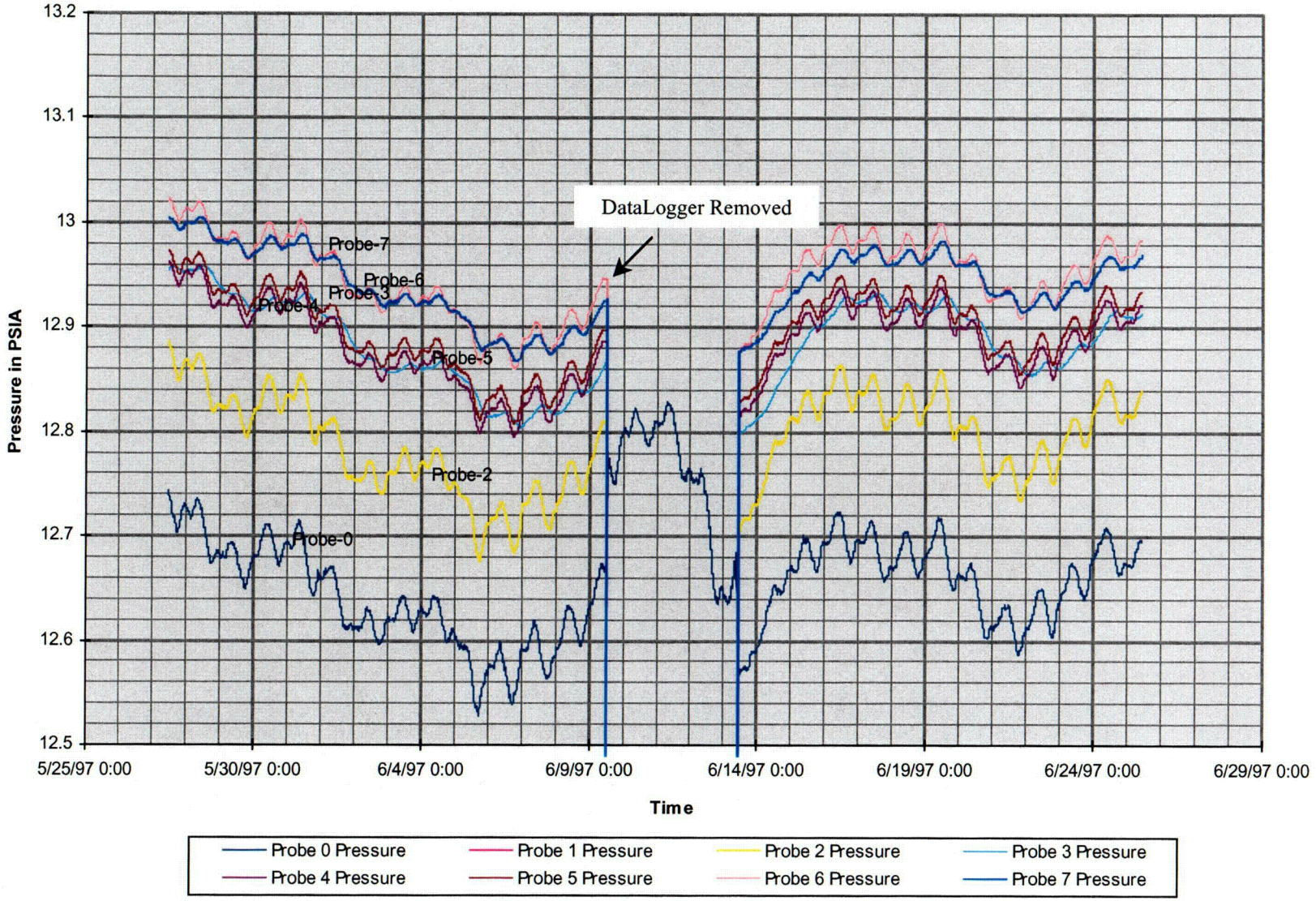

Figure 4-11 Absolute pressure for NRG-4 corrected with interpolation calibration, June 1997.

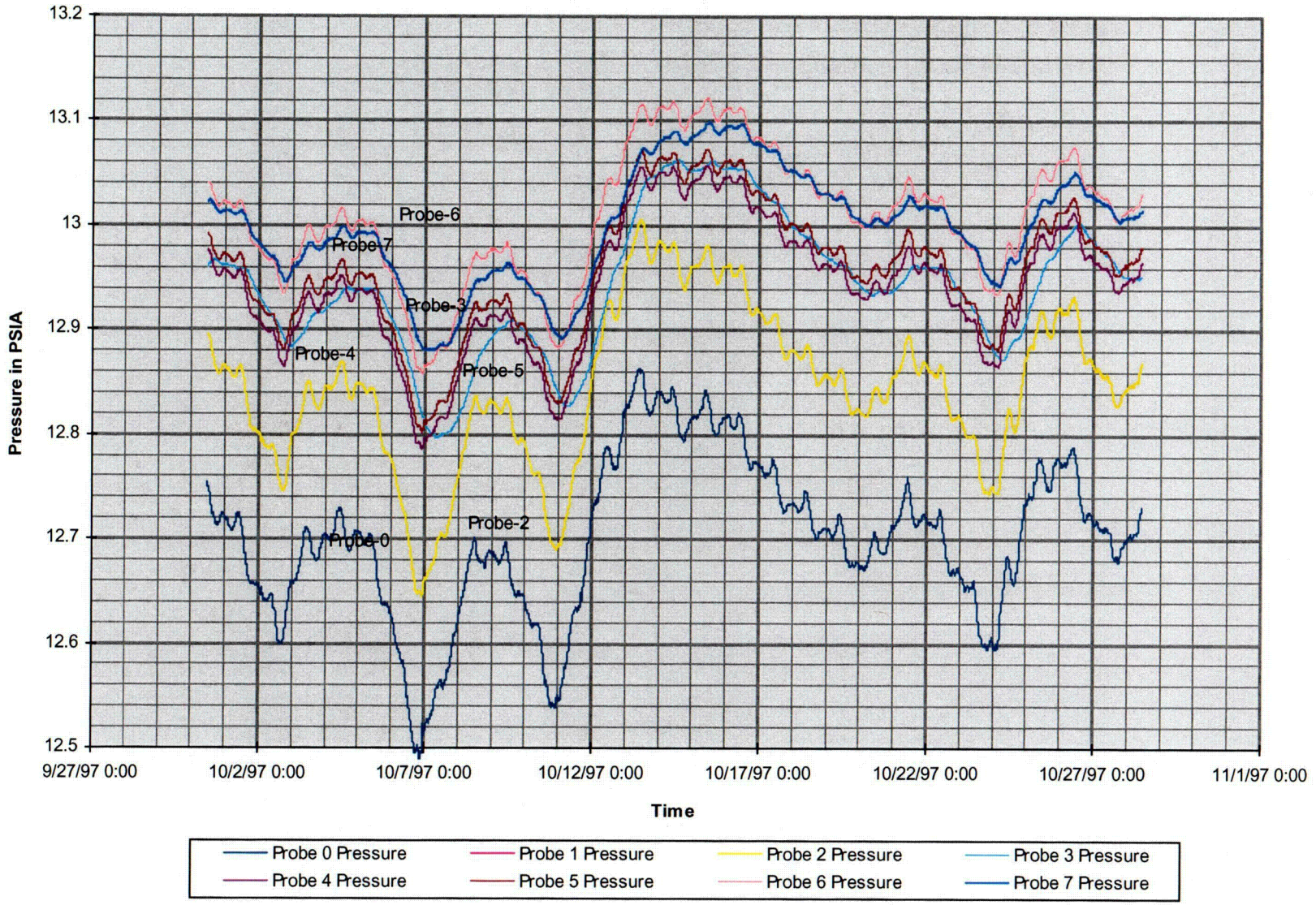

Figure 4-12 Absolute pressure for NRG-4 corrected with interpolation calibration, October 1997.

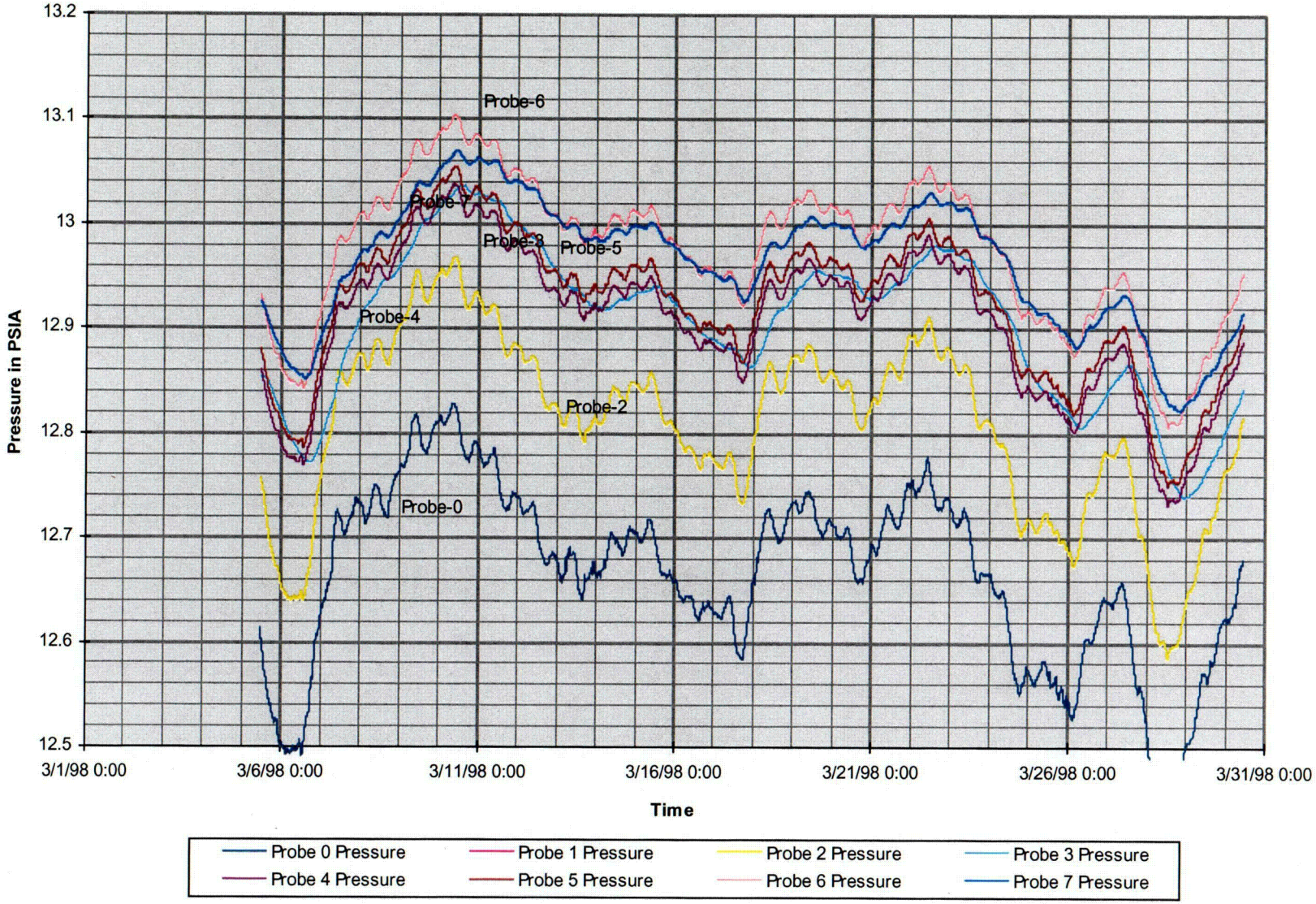

Figure 4-13 Absolute pressure for NRG-4 corrected with interpolation calibration, March 1998.

5.0 SITE HYDROCHEMISTRY

5.1 CHLORINE-36 GEOCHEMISTRY OF CUTTINGS SAMPLES FROM UE-25 ONC#1

5.1.1 INTRODUCTION

Nye County's first borehole (Stellavato, 1996; Stellavato et al., 1995) for oversight purposes was drilled in December 1994, using dual-wall, reverse circulation technology. This borehole is located approximately 793m northwest of the "C" well complex, southwest of Midway Valley, and between boreholes UE-25UZ-16 and UE-25p#1. Composite cuttings samples were collected over every five-foot interval of the borehole; we utilized mostly a 25% split of these composite samples. Emphasis for this study was placed on characterizing potential rapid transport pathways for radionuclides to the biosphere and determining if any such transport occurred at this location.

5.1.2 METHODOLOGY

Our subcontractor, Dr. Marek Zreda of the Department of Hydrology and Water Resources, University of Arizona, prepared the samples by the following procedure. Samples for ^{36}Cl were leached three times in 18-megaohm water, roughly in the proportion of 1 part of sample to 1 part of water. All leachate waters were transferred to a large beaker and combined into one sample. Then, 1 ml of chlorine isotopic spike (99% ^{35}Cl and 1% ^{37}Cl) was added to produce enough Cl for the analysis of ^{36}Cl. Chloride was then precipitated as AgCl by addition of 20 ml of 0.1M $AgNO_3$ and purified of sulfur using standard methods (Zreda et al., 1991). The ratio of ^{36}Cl to Cl ($^{36}Cl/Cl$) was measured using accelerator mass spectrometry (Elmore et al., 1979) at the Prime Laboratory, Purdue University.

5.1.3 RESULTS

Table 5-1 lists the results to date of chlorine-36 analyses of leachate from rock cuttings samples from UE-25 ONC#1. There are some duplicate analyses for quality assurance purposes (labeled "A" and "B" in Table 5-1). For several samples (labeled "coarse" and "fine" in Table 5-1), the coarse and fine fractions were separated from the composite cuttings and analyzed separately. The coarse fraction always had the higher $^{36}Cl/Cl$ ratio suggesting that the finer fraction had relatively less ^{36}Cl due to rupturing of fluid inclusions and exposure of broken mineral grains (during drilling). Both of these processes present in-situ chlorine to the laboratory leaching solutions which is "older", and thus more decayed, than that deposited by more recent infiltrating waters.

Figure 5-1 includes all of the data collected to date plus unpublished data (personal communication, Dr. June Fabryka-Martin, Los Alamos National Laboratory, 1998). Data are plotted at the top of the five-foot interval for that composite cuttings sample. In fact, the highest measured $^{36}Cl/Cl$ ratio (about 825E-15) for cuttings from this borehole is one of Dr. Fabryka-Martin's samples at about 1,400 feet depth in the upper Prow Pass (labeled "PP" on Figure 5-1).

5.1.4 CONCLUSIONS

The first leachate water produced from coarse samples gave $^{36}Cl/Cl$ values in the range from 290E-15 to 686E-15. This is typical of the natural $^{36}Cl/Cl$ background expected in precipitation in this region during the last 10,000 years (Fabryka-Martin et al., 1997) and the measured value of ~500E-15 in pore water at this location (Fabryka-Martin et al., 1996). The observed range is due to natural temporal variability of $^{36}Cl/Cl$ in precipitation and dry fallout. This variability is caused by the variable strength of the geomagnetic field, which results in corresponding changes in the production rates of ^{36}Cl and other cosmogenic isotopes.

No bomb-pulse chlorine has been detected thus far, but we are awaiting results of ^{36}Cl analyses on more cuttings samples.

5.2 GAS SAMPLING FROM UE-25 ONC#1

The purpose of the gas sampling is to:

- Estimate the ages of the gases in the vadose zone in UE-25 ONC #1 and their relationship with the ages of the water obtained from other boreholes at Yucca Mountain that could help evaluate the percolation and recharge at the site.

- Understand the transport mechanism governing gaseous migration in the vadose zone at this site.

- Evaluate the effect of tunneling on the repository horizon.

The Exploratory Studies Facility (ESF) tunnel has been approaching the area of UE-25 ONC#1. It broke through at the South Portal on May 20, 1997. The tunnel is a boundary condition for temperature, pressure, humidity, and environmental isotopes. As the tunnel penetrated the rocks in the repository horizon, the air in the tunnel became an avenue for communication between the air in the geologic formations at the repository horizon and the atmosphere outside the tunnel. Diurnal variations in temperature and pressure observed in the tunnel correspond with the outside atmospheric fluctuations. Pressure and temperature responses that have been observed in various unsaturated zone boreholes, including UE-25 ONC#1, can be attributed to the presence of the ESF tunnel. It is suspected that if air pressure responses are detected at relatively long distances away from the tunnel, fracture pathways for migration of gases may exist. Therefore, it may be possible to detect existing gaseous chemicals in the atmospheric air introduced into the repository horizon through the tunnel.

Gas samples have been collected three times from UE-25 ONC#1. The first sampling was performed in October 1996 and consisted of sampling for carbon 14, tritium, and chlorinated fluorocarbons (CFC). The detection limit for the CFC was selected at too high a value in the first preliminary sampling effort. In June 1997, a second set of samples were collected for the same compounds but pertinent environmental gases were analyzed for at a much lower detection limit. During the third sampling event that took place in April 1998, the same set of environmental gases were analyzed for. In this third sampling effort, only two zones near the fault zone were selected for time-dependent carbon-14 sampling. The time-dependent carbon-14 sampling was performed to resolve issues that were raised in previous sampling efforts.

The results of the first sampling effort were presented in previous reports (Multimedia Environmental Technology, Inc., May 1997, this is the last annual report and Multimedia Environmental Technology, Inc. February 1997, this is the gas sampling report) and will not be repeated here except for comparison purposes. The results of the last two sampling reports are discussed below.

5.2.1 JUNE 1997 GAS SAMPLING

The samples collected in June 1997 were intended to complete the background sampling of compounds that could not be sampled during the October 1996 sampling and also to verify some of the values that were reported in the earlier report (Multimedia Environmental Technology, Inc., February, 1997). The current plan is to repeat the environmental gas sampling on an annual basis to monitor the changes in environmental chemicals in UE-25 ONC#1 that could potentially be attributed to the introduction of these chemicals to the repository horizon by the ESF tunnel. The results of these sampling rounds and subsequent analysis of data will be used to evaluate the conductive nature of the repository host rock. Gas-transport parameters may be estimated from analysis of the data and may be used in evaluation of the potential for transport of gaseous radionuclides from the

repository to the accessible environment. These data will also be used to evaluate the ability of a naturally ventilated repository to perform safely and adequately. Sampling and testing of UE-25 ONC#1 air is expected to provide information about the pneumatic and thermal conductivity as well as the diffusive and dispersive nature of the rock.

Environmental chemicals such as fluorocarbons and isotopes such as ^{14}C, ^{13}C, and ^{3}H are introduced through the tunnel air as a constant source. The tunnel air has near atmospheric chemical composition. These chemical species and isotopes enter the unsaturated zone (UZ) with advection of the atmospheric air caused by the changes in the air pressure of the tunnel. These gases are transported in the UZ by the advective, dispersive, and diffusive processes.

Once the pre-excavation conditions are established at the UE-25 ONC#1 site, the changes in the chemical composition of the pore gas with time may be analyzed to evaluate the arrival of these environmental tracers in UE-25 ONC#1. With adequate data, transport properties of the rock mass between the tunnel and UE-25 ONC#1 may be evaluated. The volume of rock affected by this test is the largest that has ever been tested at the Yucca Mountain site.

5.2.1.1 APPARATUS AND SAMPLING PROCEDURES

The sampling apparatus is schematically shown in Figure 5-2 (also see Photograph 5-1). Detailed sampling procedures are outlined in Nye County's Technical Procedure 9.40 entitled "Gas Sampling Procedure of UE-25 ONC#1 and other Westbay Instrumented Wells". A brief description follows.

The Westbay access tube was fitted with a vacuum-tight plug (Figure 5-2) during sampling. By applying vacuum in the access tube through this plug, sampling was performed at selected depth intervals. The surface attachments consisted of:

1. Tritium sampling unit (TSU).

2. The CFC and organic compound canister.

3. The Tedlar bag vacuum purging and sampling (TBVPS) unit.

4. Flow metering unit (FMU).

5. Temperature probe.

6. Vacuum pump (VP).

The first four units had by-pass valves that were used during purging of the sampling zone. Flow rates in excess of 2 ft^3/min (0.06 m^3/min) were used during purging for 1.5 to more than 12 hours. The duration of flow was calculated to be sufficient to evacuate the entire string, the entire annulus between the packers, and a radius of at least 2.5 feet into the formation, based on an average air-filled porosity of 10 percent. Assuming air-filled porosity of 10 percent is very conservative. Actual air-filled porosity is less than 1 percent for the formations sampled. Therefore, in some cases the formation may have been purged to a radial distance of up to 25 feet around the borehole prior to sampling.

In addition to the sampling apparatus, the down-hole Westbay MOSDAX probes were set as monitoring ports at various intervals during purging. The pressure and temperature data were used to calculate pneumatic conductivity of the formations sampled.

As soon as the purging process was completed, the by-pass valve for the CFC canister was closed and the valve to the canister opened. Because the canister was already under vacuum from the laboratory, it automatically filled with the gas from the line. Then the Tedlar bags were filled (depending on the zone of interest, one or two 10 liter bags were filled), the by-pass valve for the TSU was shut and air was allowed to flow through the Tritium Microsieve Sampling Cylinder (TMSC). All the TMSCs were weighted, prepared, and sealed in the laboratory prior to field sampling. The by-pass valve at the FMU was also closed to allow

for monitoring of the flow rate. A minimum of one hour of flow was allowed to occur through the TMSCs at an approximate rate of 1 ft^3/min (0.03 m^3/min). This time duration allowed entrapment of between 50 and 70 grams of water in the molecular sieve.

Once Tritium sampling was completed, the TMSC was disconnected and shipped to the laboratory in a cooler.

5.2.1.2 CHEMICAL SAMPLING ZONES

The Westbay access tube can be opened at nine locations in UE-25 ONC#1 (Figure 5-3) using sliding sleeves that, once opened, expose slotted sections of the access tube. Each of the six vertical slots in a section is 1.75 in (4.5 cm) long and 0.5 in (1 cm) wide. By opening each one of the sliding sleeves, a packed-off section of the borehole can be sampled by applying a vacuum to the inside of the access tube.

Seven of the nine access tube port locations were used for sampling during testing performed from June 3 through June 12, 1997. The locations of four of these screens are identified by a "GS- " prefix in Figure 5-3. Samples GS-1, GS-2 and GS-2A were selected to be near the fault zone. GS-5 was selected to be in the Tiva Canyon Welded Unit (TCWU) above the Paintbrush Tuff Nonwelded Unit (PTNU). Additionally, samples were taken from access tube screen 8 in the PTNU and screens 1 and 2 below the water table. Samples of the atmosphere just above the top surface of UE-25 ONC#1 were also collected.

5.2.1.3 RESULTS OF JUNE 1997 GAS SAMPLING

A summary of the tests and sampling performed in UE-25 ONC#1 during June of 1997 is shown in Table 5-2. Table 5-3 tabulates the results of all the chemical analyses excluding Carbon-14. Figure 5-4 is a plot of all the chemical analyses except for the isotopic analyses. Figures 5-5 through 5-8 show individual groups of chemicals. Figures 5-9 and 5-10 are the results of O-18 and Deuterium

analyses. The tunnel data are also shown in these figures when available at depths of 100 and 200 feet. These depths were arbitrarily chosen to show the tunnel data because there are no sampling ports in UE-25 ONC#1 at these depths.

Figure 5-5 shows the distribution of methane and carbon oxides. Concentrations of both methane and carbon dioxide are similar for the atmosphere and the tunnel. Methane is depleted at a depth of 1225 feet in UE-25 ONC#1. On the other hand, carbon dioxide shows an increasing trend to a depth of 700 feet. A sharp decline is observed near the fault zone below which an increase in carbon dioxide is observed. The increase in carbon dioxide with depth has been observed in other boreholes at Yucca Mountain. However, the decrease at the fault zone seems to be an anomaly that requires explanation.

A plot of the chlorinated hydrocarbons with depth is shown in Figure 5-6. Trichloroethane (TCA) concentration appears to be only elevated in the tunnel and absent in the fault zone. Its presence below the fault zone is attributed to the sample container. Tedlar bags allow slight diffusion of some gases (especially volatile organic compounds) through their plastic wall. Therefore, TCA is believed to be absent in the vadose zone of UE-25 ONC#1 and is considered to be a good candidate tracer for monitoring any tunnel air interaction with the subsurface environment. However, TCA is a compound that is highly sorbed on other organic matter in the vadose zone and may not be a conservative tracer.

Figure 5-7 is a plot of the concentration of chlorinated fluorocarbon compounds (CFCs) with depth. Concentrations in the tunnel are similar to the atmospheric concentrations as expected. A decrease in concentration with depth has also been observed elsewhere at Yucca Mountain. The increase in F11 and F12 at a depth of 1225 feet, which is below the fault zone, is attributable to the Tedlar bag as can be seen by comparison with the results of the sample in the canister from the same zone. However, in the upper part of the fault zone, slight deviation from the linear trend can be seen in all three compounds.

Figure 5-8 presents the concentration of nitrous oxide with depth. The concentration levels of nitrous oxide in the tunnel are slightly lower than the atmospheric concentration levels; however, they are similar to the concentration levels in UE-25 ONC#1 at Topopah Springs horizon. Concentration values of nitrous oxide appear to increase noticeably near the fault zone. The decline in the Tedlar bag sample below the fault zone is attributable to sample contamination with atmospheric air by diffusion through the wall of the bag. Nitrous oxide is present in the atmosphere and is believed to be present in elevated levels in groundwater due to biological activities. Its elevated concentration in the fault zone is currently under investigation. One possibility is diffusion from the water table.

Figure 5-9 is a plot of Deuterium and O-18 ratios with depth and Figure 5-10 is a plot of their correlation. The bottom two samples are groundwater samples and the remainder is the results from condensation collected from the vadose zone. Both isotopes appear to be lighter in the vadose zone; this is attributed to potential fractionation of these isotopes during flow of the air from deeper zones. Figure 5-10 shows that the water samples are very similar in their composition of these isotopes to the perched waters at the site.

Table 5-4 lists the results of Carbon-14 isotope sampling. Testing was performed to measure the age of the Carbon-14 isotope in the unsaturated zone and in the groundwater of UE-25 ONC#1. A plot of the apparent age of the groundwater based on this isotope versus depth is shown in Figure 5-11. Although these ages are corrected for ^{13}C ratios, they are not corrected for the dead carbon in the groundwater. Personal communication with Ed Kwicklis of the U.S. Geological Survey indicates that the groundwater ages may be 2000 to 4000 years overestimated. However, the activities reported from UE-25 ONC#1 compare very well with the Yucca Mountain database. Carbon-14 apparent ages support a systematic trend for the ages in the unsaturated zone as expected. The age gradually increases until the fault zone is reached. At this point, the age of the

Carbon-14 drops roughly more than 1000 years. Through the fault zone and until the water table is reached, the age progressively increases again. The ages for both measurements taken from the groundwater are about the same.

Based on ^{13}C values, atmospheric contamination of all other samples is minimal, if any. The only time that atmospheric air may have contacted the samples is during removal from the TBVPS; however, the inlet into the bag is very small and the amount of atmospheric air that can be accidentally introduced into the bag is less than 0.1 percent of the volume of the sample.

Figures 5-12 and 5-13 compare UE-25 ONC#1 sampling in 1996 and 1997 with UZ-1, UZ-14 and UZ#16 values for Carbon-14 and ^{13}C (Yang et al., 1996). Comparison of the data from UE-25 ONC#1 in June 1997 sampling with those from UZ-1 reveals significant differences and some similarities in the carbon isotope signatures. The isotopic signatures in TCWU are not similar between the UE-25 ONC#1 and the other boreholes. In UE-25 ONC#1, the ^{14}C activity is about 20 to 40 percent less than that of the other boreholes at the same vertical distance from the top of the TCWU. Carbon-14 activity in UZ-1 is 33 percent lower than the activity at an equivalent depth in UE-25 ONC#1 (GS-4 sample). If the value of GS-4 is representative of the conditions in UE-25 ONC#1, the apparent age of the gas at this level would be about 500 years. This is considerably younger than any apparent age reported for UZ-1 borehole below a depth of 100 feet (30 m). Conversely, the activity of C-14 in the Topopah Springs through the fault zone is about the same as that in UZ-1. The activity of GS-2A sample is less than 10 percent lower than that of the equivalent horizon in UZ-1. This sample is not likely to have been contaminated with the atmosphere due to its much heavier ^{13}C (-6.0) ratio as compared with the atmospheric ^{13}C (about -9 at Yucca Mountain). However, it is possible that fractionation may have occurred as a result of preferential diffusion of lighter carbon isotope through the wall of the Tedlar bag. The C-14 activity in Calico Hills unit is similar for UE-25 ONC#1 and UZ#16.

GS-1 sample is in the Calico Hills Nonwelded Unit and is on the hanging wall of the fault zone. The apparent younger age of this sample in October 1996 could not be confirmed and a much older age was reported in the June 1997 sample from the same zone. This younger age contradicts the data from other boreholes and the conceptual model of Montazer and Wilson (1984). However, the high value of ^{13}C (-3.6) in October 1996 was confirmed with values of -5.7 and -6.0 in the June 1997 sampling event. Such ranges of ^{13}C have not been reported anywhere else at Yucca Mountain. These values are usually associated with the presence of carbonates of marine origin. The reason for their presence at the fault zone is not clear at this time. According to Al Yang of the U. S. Geological Survey (personal communication, 1997), the Calico Hills Unit is not known to have an abundance of carbonates. Because of the heavy signature of the ^{13}C, atmospheric contamination of the samples is ruled out. A possible explanation for the discrepancy between the results of the two sampling events is postulated to be the difference in the zone of influence. In the June 1997 sampling event, a larger volume of air was purged and, therefore, the sample represents a larger area around the borehole. The October 1996 sample was taken only after 2.5 hours of purging. The smaller purged volume may represent the fault characteristic better than the larger sample. Therefore, it may be possible that the ^{13}C signature of the June 1997 sample is due to mixing of air from the fault zone with the air from the surrounding formation, which has a much lighter ^{13}C signature. The Carbon-14 activities also represent an average between the fault zone and the overall formation characteristics. If this postulation is assumed correct, the October 1996 Carbon-14 activity of the fault zone may be interpreted to indicate the presence of a younger water in the fault zone. Sampling using incremental increases in volume of purged air performed in April 1998 has clarified this uncertainty (see the following section).

5.2.2 APRIL 1998 GAS SAMPLING

Background conditions had been established at the UE-25 ONC#1 site during previous sampling events. Therefore, the sampling in April 1998 was focused on detecting changes in the chemical composition of the gas with time needed to evaluate the arrival of these environmental tracers in UE-25 ONC#1 from the ESF tunnel. The second objective of this sampling effort was to evaluate the cause of discrepancy between the results of the two previous sampling events in carbon-14 ages. Samples collected during April 1998 were analyzed for CFC/organic chemicals and ^{14}C only.

5.2.2.1 APPARATUS AND SAMPLING PROCEDURES

The sampling apparatus used during the April 1998 sampling event is schematically shown in Figure 5-14. This apparatus was slightly different from the previous sampling setup as briefly described in the following.

The Westbay access tube was fitted with a vacuum tight plug (Figure 5-14) during sampling. By applying vacuum in the access tube through this plug, sampling was performed at selected depth intervals. The surface attachments were slightly different as compared to previous sampling events. They consisted of:

1. The CFC and organic compound canister.
2. The Tedlar bag vacuum purging and sampling (TBVPS) unit (used for ^{14}C sample collection).
3. Vacuum pump (VP).

The first two units had by-pass valves that were used during purging of the sampling zone. Flow rates in excess of 2 ft^3/min (0.06 m^3/min) were used during

purging for 0.5 to more than 16 hours for ^{14}C samples and for 4 hours for CFC samples.

In addition to the sampling apparatus, the down-hole Westbay MOSDAX probes were set as monitoring ports at various intervals during purging conducted on April 22 and 23. Pressure and temperature data were collected on the 22nd and on the subsequent day, April 23rd, during sampling at screen #4. These data were used to calculate pneumatic conductivity of the formation sampled.

As soon as the purging process was completed, the by-pass valve for the CFC canister was closed and the valve to the canister opened. Because the canister was already under vacuum from the laboratory, it automatically filled with the gas from the line. The same process was used during collection of ^{14}C samples. Tedlar bags were purged three times before filling (one 10-liter Tedlar bag was filled for each ^{14}C sample collected).

5.2.2.2 CHEMICAL SAMPLING ZONES

As described in the previous section concerning the June 1997 gas sampling event, the Westbay access tube can be opened at nine locations in UE-25 ONC#1 (Figure 5-15) using sliding sleeves that, once opened, expose slotted sections of the access tube. Seven of the nine access tube port locations (screens) were used for sampling during testing performed from April 20th through April 30th, 1998. Sample collection locations or pumping ports (screens #3 through #9) are indicated in Figure 5-15. Samples collected at screens #3, #4 and #5 were selected to be near the fault zone. Samples collected at screens #6 and #7 were selected to be in the Topopah Springs Unit. The sample collected from access tube screen #9 was selected to be in the Tiva Canyon Welded Unit (TCWU) above the Paintbrush Tuff Nonwelded Unit (PTNU). Additionally, a sample was taken from access tube screen #8 in the PTNU. CFC samples were collected at all seven of the screen locations after purging the borehole for four hours for each screen sampled. An atmospheric CFC sample was also collected just above the

top surface of UE-25 ONC#1. ^{14}C samples were collected at only screen #3 and screen #7. A total of six ^{14}C samples were collected at each of these screens. ^{14}C samples were collected at different time intervals over a period of 16 hours during which purging of the borehole continued. These samples were collected at the following intervals: ½, 1, 2, 4, 8 and 16 hours. The ambient temperature was also recorded periodically during this sampling round.

A summary of the sampling and testing performed at UE-25 ONC#1 during April of 1998 is shown in Tables 5-5 and 5-6. After sample collection, samples were packed in coolers and sent to the appropriate laboratories with accompanying Chain of Custody forms.

5.3 CONCLUSIONS AND RECOMMENDATIONS

Preliminary results from all three sampling events indicate that the sampling method used for obtaining gas samples from UE-25 ONC#1 is very efficient and produces results that seem to be comparable with results of other UZ sampling techniques that have been used at the Yucca Mountain Site. Tritium sampling results from October 1996 are confirmed with the results of the June 1997 sampling results. No bomb pulse tritium was found in the gases of the unsaturated zone. This demonstrates that there has not been a pervasive recharge event in the vicinity of UE-25 ONC#1 during the past 50 years. This is confirmed by the results of the chlorine-36 sampling of the drill cuttings (see Section 5.1). However, because the gas sampling method used averages the concentration of the isotopes from the purged volume, small and discrete fluxes in fractures may not be detectable. The young carbon-14 ages, observed in the October 1996 sampling round, were not repeatable in either one of the subsequent sampling events. In variable-time interval sampling of April 1998, it was concluded that the young ages detected in October 96 samples must have been due to preferential diffusion of the lighter carbon isotopes through the Tedlar bags. Therefore, the range of the

ages in the vadose zone at and below the TSWU is between 5000 to 8000 years. These ages represent the residence time of the pore water and not the gas ages.

Sampling of CFCs and organic compounds must be done using special canisters. No further sampling and analysis of tritium seems to be necessary.

The groundwater ages need to be corrected; however, it is not certain whether any further correction in the vadose zone C-14 ages needs to be performed. If no corrections in the vadose zone ages are made and the ages of groundwater are corrected to be 8000 to 10000 years old, then there seems to be a consistent trend in the ages from the ground surface to the groundwater in the area of the UE-25 ONC#1.

The results of the three sampling events indicated that TCA and CFC are good tracers for atmospheric diffusion of gases in the vadose zone of the Yucca Mountain. These compounds, along with the other compounds such as nitrous oxide, will be monitored in future sampling efforts. No further carbon-14 and tritium sampling seem to be necessary from UE-25 ONC#1. However, general chemistry samples from groundwater may be needed to verify the original results obtained from samples collected immediately after drilling in the saturated zone.

The fact that the diffusion of the modern gases (CFCs) into the vadose zone to depths of greater than 1200 feet is observed indicates that the Yucca Mountain vadose zone is a pneumatically open system in direct communication with the atmospheric air. The fact that the C-14 samples show depleted modern C-14 concentrations indicates that the carbon dioxide in the air of the vadose zone is in an equilibrium state with the aqueous-phase carbonates. Therefore, the C-14 activities are believed to be representative of the activities of the moisture in the rocks that are in equilibrium with the air in the vadose zone. The absence of bomb pulse tritium and chlorine-36 also supports this conclusion. If water had

moved as fast as the gases, bomb pulse tritium and chlorine-36 would have been detected. The reason that this concept may appear to contradict the observations of the bomb pulse chlorine-36 in the ESF is that the samples collected in UE-25 ONC#1 are averages of large volumes of the formation air. If discrete percolation pathways exist at this site, such as those found in the ESF tunnel, they could not be detected with this method. In any case, the results show that such discrete percolation flux pathways, if present, are very isolated and not pervasive (otherwise the systematic sampling would have detected some anomaly). It is also recommended that the results and interpretation of the chlorine-36 samples from the ESF be more carefully and thoroughly analyzed to evaluate other possible explanations for the presence of the bomb pulse at the ESF level. In general, it may be concluded that the percolation in the area of UE-25 ONC#1 is not fast despite the presence of the Bow Ridge Fault Zone.

Comparison of the CFC results from the two sampling events in April 1998 and June 1997 indicates some significant differences between the concentration of the F-12 and F113 that may be reflective of changes of chemistry in the vadose zone. However, because the analytical laboratory for the organic chemicals was different between the two events, the significance of the difference is not considered conclusive until further verification and quality assurance comparison between the two laboratories are conducted.

A preliminary observation and interpretation of the differences between the last two sampling events indicates that the fault zone must have had a significant influence in transport of the CFC to a depth of 1200 feet. Comparison between the data for the two sampling periods does not show detectable differences between the two time periods.

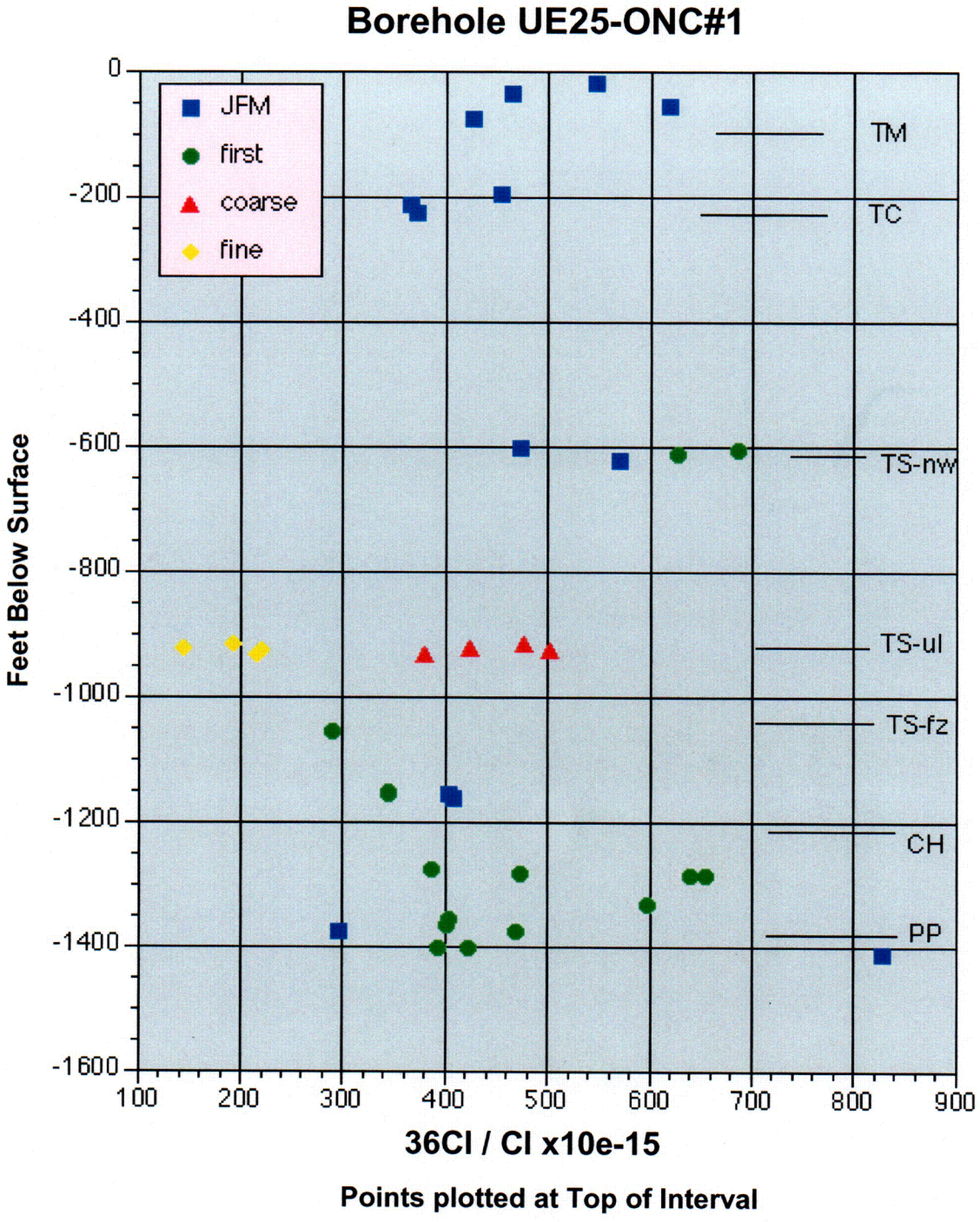

Figure 5-1 **Composite cuttings sample.**

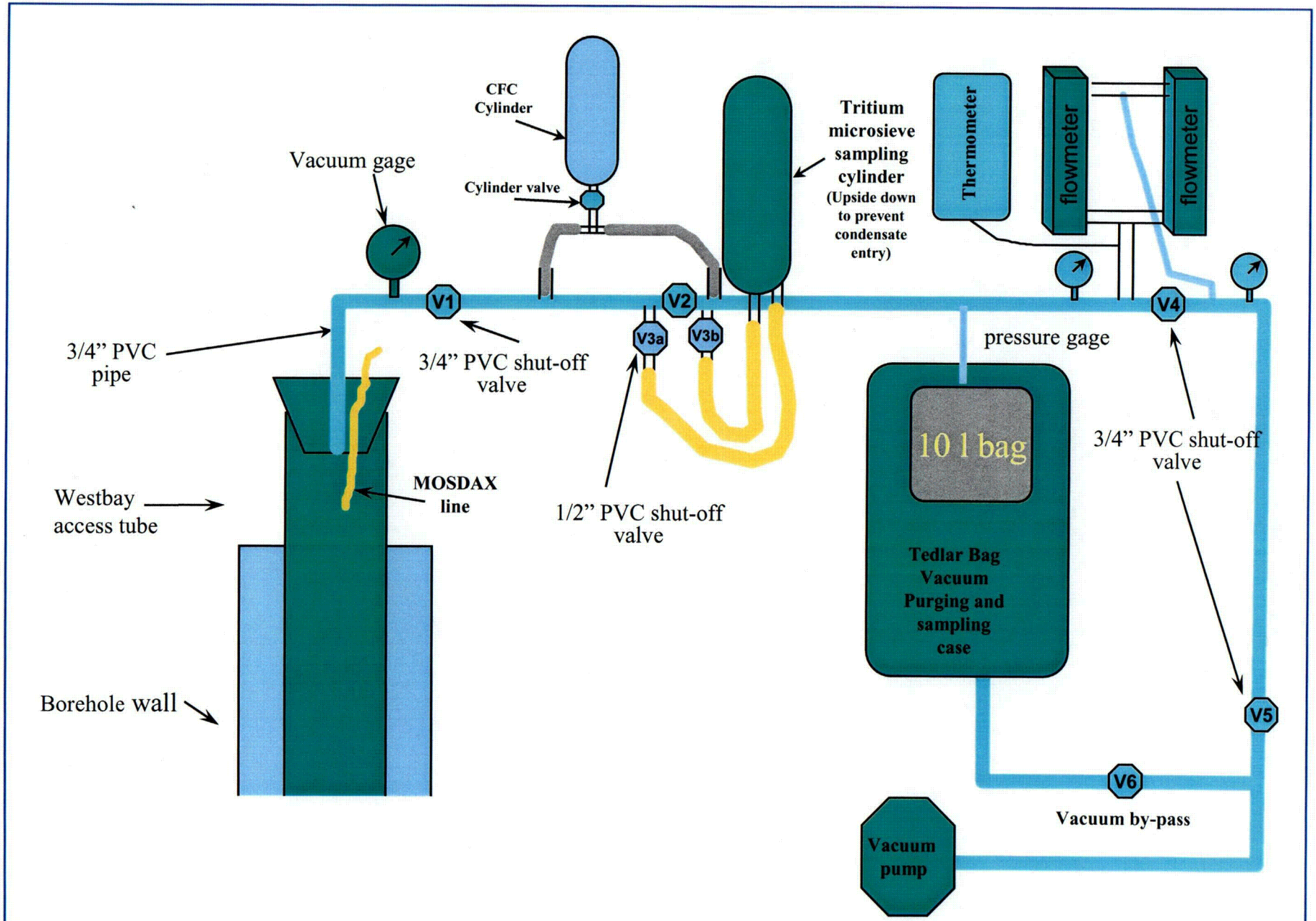

Figure 5-2 **Schematic diagram of the surface attachments for gas sampling, June 1997.**

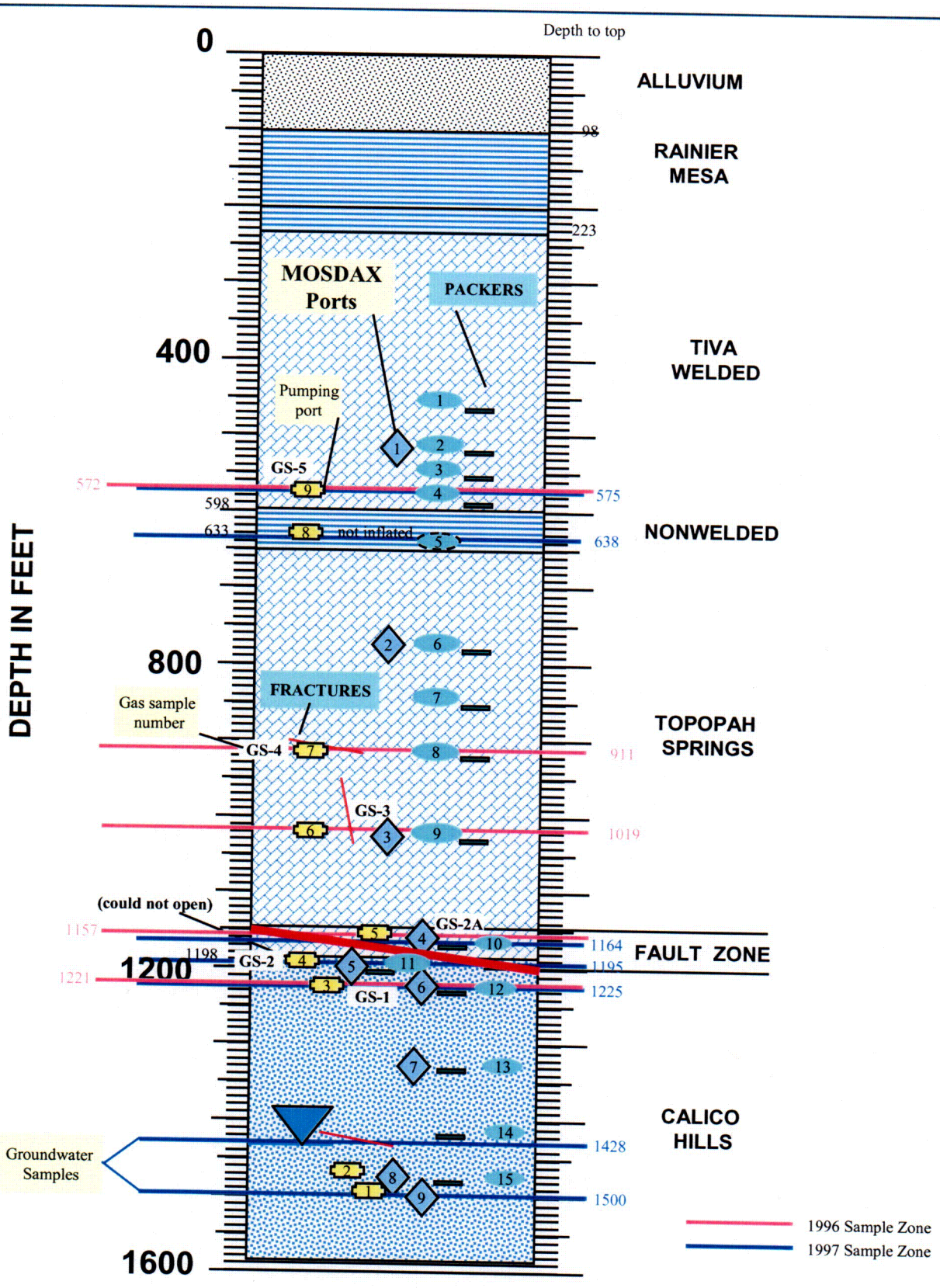

Figure 5-3 ONC#1 stratigraphy & instrumentation profile June 1997 gas sampling.

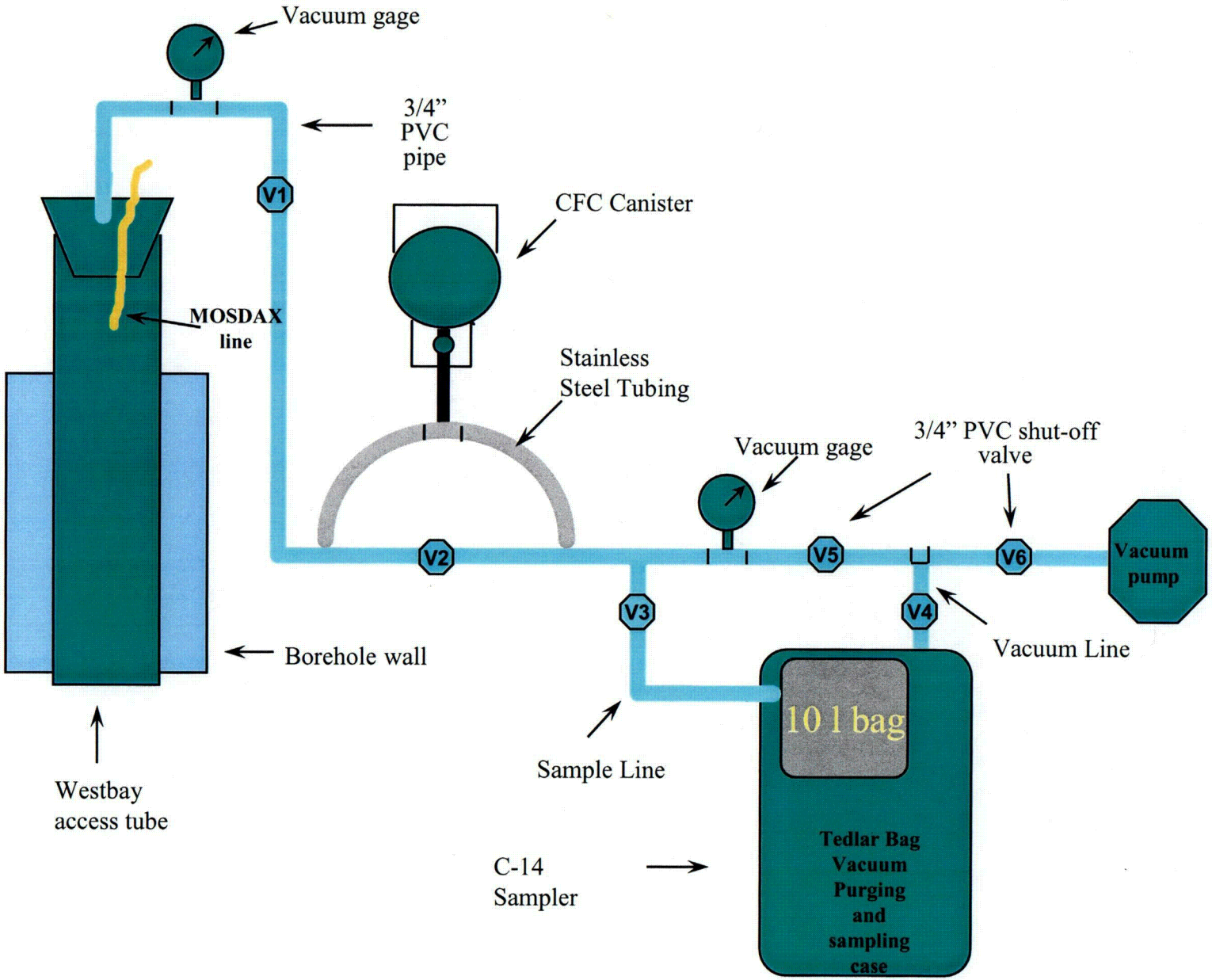

Figure 5-14 **Schematic diagram of the surface attachments for gas sampling, April 1998.**

C-17

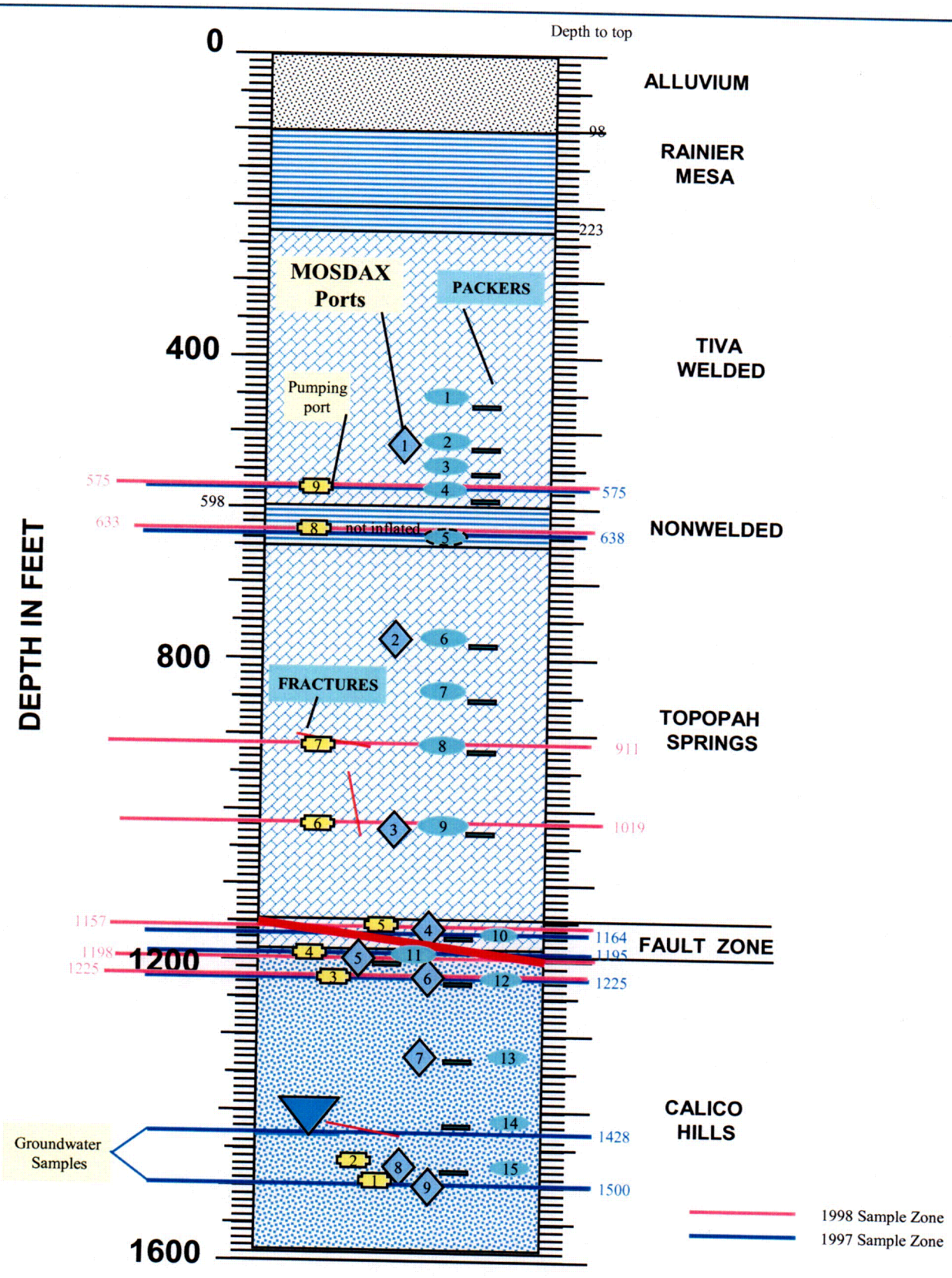

Figure 5-15 ONC#1 stratigraphy & instrumentation profile April 1998 gas sampling.

Table 5-1 Chlorine-36 Analyses of Leachates From Rock Cuttings Samples

Both total Cl and the Cl ratio were determined by AMS;
the Cl ratio was corrected for the 35Cl spike.

Depth Interval (feet)	Leach	Stratigraphy	Total Cl (ppm)	36Cl/Cl x10e-15
608-613	first	bedded tuff, Paintbrush Tuff	4.36	686
613-618	first	bedded tuff, Paintbrush Tuff	4.05	628
618-623	first	non-welded Topopah Springs	2.71	465
918-923	coarse	u. lithophysal, Topopah Springs	0.93	479
918-923	fine	u. lithophysal, Topopah Springs	0.26	194
923-928	coarse	u. lithophysal, Topopah Springs	0.99	426
923-928	fine	u. lithophysal, Topopah Springs	0.21	145
928-933	coarse	u. lithophysal, Topopah Springs	0.99	504
928-933	fine	u. lithophysal, Topopah Springs	0.19	220
933-938	coarse	u. lithophysal, Topopah Springs	1.73	380
933-938	fine	u. lithophysal, Topopah Springs	0.31	217
1,058-1,063	first	m. lithophysal, Topopah Springs	1.19	290
1,153-1,158	first, A	Topopah Springs fault zone	0.32	344
1,153-1,158	second	Topopah Springs fault zone	0.5	101
1,158-1,163	second	Topopah Springs fault zone	0.28	118
1,158-1,163	first	Topopah Springs fault zone	1.16	345
1,278-1,283	first	Calico Hills	3.2	387
1,283-1,288	first	Calico Hills	0.22	474
1,288-1,293	first, A	Calico Hills	1.37	656
1,288-1,293	first, B	Calico Hills	2.09	641
1,333-1,338	first	Calico Hills	2.09	599
1,358-1,363	first	Calico Hills	4.3	405
1,368-1,373	first	Calico Hills	7.67	401
1,378-1,383	first	Prow Pass member, Crater Flat tuff	2.38	469
1,403-1,408	first, A	Prow Pass member, Crater Flat tuff	0.87	424
1,403-1,408	first, B	Prow Pass member, Crater Flat tuff	2.07	393

Note: letter after leach indicates a sample split; second leach is after additional crushing.
Coarse and fine refer to the two size fractions of a cuttings sample as received.
(coarse + fine size fractions = whole sample)

Table 5-1 Chlorine-36 Analyses of Leachates From Rock Cuttings Samples

Both total Cl and the Cl ratio were determined by AMS;
the Cl ratio was corrected for the 35Cl spike.

Depth Interval (feet)	Leach	Stratigraphy	Total Cl (ppm)	36Cl/Cl x10e-15
608-613	first	bedded tuff, Paintbrush Tuff	4.36	686
613-618	first	bedded tuff, Paintbrush Tuff	4.05	628
618-623	first	non-welded Topopah Springs	2.71	465
918-923	coarse	u. lithophysal, Topopah Springs	0.93	479
918-923	fine	u. lithophysal, Topopah Springs	0.26	194
923-928	coarse	u. lithophysal, Topopah Springs	0.99	426
923-928	fine	u. lithophysal, Topopah Springs	0.21	145
928-933	coarse	u. lithophysal, Topopah Springs	0.99	504
928-933	fine	u. lithophysal, Topopah Springs	0.19	220
933-938	coarse	u. lithophysal, Topopah Springs	1.73	380
933-938	fine	u. lithophysal, Topopah Springs	0.31	217
1,058-1,063	first	m. lithophysal, Topopah Springs	1.19	290
1,153-1,158	first, A	Topopah Springs fault zone	0.32	344
1,153-1,158	second	Topopah Springs fault zone	0.5	101
1,158-1,163	second	Topopah Springs fault zone	0.28	118
1,158-1,163	first	Topopah Springs fault zone	1.16	345
1,278-1,283	first	Calico Hills	3.2	387
1,283-1,288	first	Calico Hills	0.22	474
1,288-1,293	first, A	Calico Hills	1.37	656
1,288-1,293	first, B	Calico Hills	2.09	641
1,333-1,338	first	Calico Hills	2.09	599
1,358-1,363	first	Calico Hills	4.3	405
1,368-1,373	first	Calico Hills	7.67	401
1,378-1,383	first	Prow Pass member, Crater Flat tuff	2.38	469
1,403-1,408	first, A	Prow Pass member, Crater Flat tuff	0.87	424
1,403-1,408	first, B	Prow Pass member, Crater Flat tuff	2.07	393

Note: letter after leach indicates a sample split; second leach is after additional crushing.
Coarse and fine refer to the two size fractions of a cuttings sample as received.
(coarse + fine size fractions = whole sample)

Table 5-2 ONC#1 Testing and Sampling

June 2 to June 13, 1997

VACUUM TEST NUMBER	Ground Water	Ground Water	CFC - Atmosphere	1	2	3	4	5
TEST START DATE	03-Jun-97	03-Jun-97	03-Jun-97	04-Jun-97	09-Jun-97	10-Jun-97	11-Jun-97	12-Jun-97
DEPTH (feet)	1500	1428	0	1195	1164	1225	575	638
ZONE TESTED								
Screen	-	-	ATMOS	4 (GS-2)	5 (GS-2A)	3 (GS-1)	9 (GS-5)	8
Test Port	Port 15.2	Port 14.1	-	Port 5	Port 4	Port 6	NONE	Port 2
Serial #	-	-	-	1814	1812	1815	None	1810
MONITORING PORTS								
ABOVE	-	-	-	Port 4	Port 3	Port 5	None	Port 1
Serial #	-	-	-	1812	1811	1814	None	1818
BELOW	-	-	-	Port 6	Port 5	Port 7	None	None
Serial #	-	-	-	1815	1814	1816	None	-
HANGING MOSDAX PROBES								
Serial #	-	-	-	1818	1818	1818	None	1811
Serial #	-	-	-	1810	1810	1810	None	-
Serial #	-	-	-	1811	-	1811	None	-
Serial #	-	-	-	-	-	1812	None	-
DATALOGGER USED	None	None	None	ONC1	NRG4	ONC1	None	ONC1
SAMPLES COLLECTED								
CFC Stainless Cylinder	-	-	#WE-4	D-112, ONC1-CFC-2,060597-2	R-18, ONC1-CFC-2,060997-2A	-	-	-
CFC bag	-	-	-	-	-	ONC1-CFC-3, 6/11/97	ONC1-CFC-9-1,6/12/97	ONC1-061397-CFC
C-14	060397b2.wat	060397b7.wat	-	ONC1-C14-2,6/5/97	ONC1-C14-2A,6/9/97	ONC1-C14-3, 6/11/97	ONC1-C14-9-1, 6/12/97	ONC1-C14-8-3, 6/13/97
Tritium. Sieve	-	-	-	#543, ONC#1-TRI-2, 6/5/97	-	-	-	#739, ONC#1-061397T1
Tritium Condensate	-	-	-	-	ONC1-ZN5-GS-2A-OD-2	-	-	ONC#1-061397-T2
O-18 Condensate	060397b3.wat, 060397b4.wat	060397b6.wat, 060397b5.wat	-	060597b1.wat	ONC1-ZN5-GS-2A-OD-1	061197b1.wat	ONC1-O18-9-1,6/12/97	ONC1-061397-OD-1

6.0 WELL TEST ANALYSIS RESULTS

6.1 BACKGROUND

Well test analysis by the Nye County Nuclear Waste Repository Project Office during the period May 1, 1997 to May 1, 1998, consisted of the following activities:

1. An analysis of the pressure response of Well UE-25 ONC#1 to atmospheric pressure pulses through natural and man-made pathways, and

2. An analysis of vacuum tests conducted in Well UE-25 ONC#1

These activities are discussed in detail in the following sections.

6.2 UE-25 ONC#1 RESPONSE TO ATMOSPHERIC PRESSURE PULSES

6.2.1 INVESTIGATIVE ACTIVITIES

The Nye County Nuclear Waste Repository Project Office installed instruments in borehole UE-25 ONC#1 to monitor the pressure at various levels at Yucca Mountain, and to identify the response to atmospheric conditions and activities at the project. The well has ten probes to monitor pressure and temperature at various depths. The pressure response from March 28, 1996 through March 24, 1997 was analyzed.

6.2.2 METHODOLOGY

The original objective of the analysis was to determine whether pressure transients in UE-25 ONC#1 caused by the Exploratory Studies Facility (ESF) could be analyzed using conventional pulse test analysis techniques. The ESF tunnel broke

through the non-welded unit on June 18, 1996. After reviewing the observed response, it was determined that the effect of the tunnel could not be accounted for with a one-dimensional linear or radial flow model (Section 6.2.2.1).

Because the various zones at Yucca Mountain are in pressure communication with each other through a complex system of natural fractures and/or faults or other features, the pressures recorded by the different probes were compared using linear regression between the pressure response of adjoining probes to evaluate the degree of similarity in the pressures (Section 6.2.2.2).

To more clearly identify the various components associated with the atmospheric pressure changes, a Fourier analysis was also conducted to separate the parts of the data that are caused by each particular frequency. The basic consideration in Fourier analysis is that the function or data being analyzed is made up of a series of sinusoidal terms (sine and cosine functions) of various frequencies and strengths. The frequency refers to how often each particular term repeats, as for example daily, hourly, or yearly. The strength, or amplitude, of each term refers to the magnitude of its contribution to the total. Terms with large amplitude contribute a large amount to the pressure, while terms with small amplitudes have little effect. Two methodologies focusing on different aspects of the periodic functions were used for the Fourier analysis: a standard Fourier series expansion of the data (Section 6.2.2.3), and a Lomb analysis (Section 6.2.2.4).

6.2.2.1 CONVENTIONAL PULSE TEST ANALYSIS

A pulse test consists of producing (or injecting) into one well for a period, then stopping for a while, then resuming production, then halting, etc. The response is monitored at an adjacent observation well. From the time lag between the pulsing of the active well and the time and magnitude of the observation well response, it is possible to determine the permeability and storage constant (ϕch) of the porous medium (Earlougher, Jr., 1977). Atmospheric pressure changes provide a "natural pulse test" at Yucca Mountain.

Originally, it was thought that the effect of the ESF tunnel breaking through the non-welded unit might be analyzed in this fashion. Figure 6-1 shows the atmospheric pressure and Probe 3 response around the time of tunnel breakthrough. Probe #3 in UE-25 ONC#1 is located at a depth of 1029 feet in the Topopah Springs Unit below the Paintbrush Nonwelded Unit (the PTn). The response of Probe #3 changed after the ESF tunnel breakthrough. Prior to breakthrough, Probe #3 responded to the atmospheric pressure changes (recorded by Probe #0 at the surface) with a time lag of about 1 day. About half of the overall atmospheric pressure changes were evident in Probe #3, except the higher frequency (short period) daily spikes were "smoothed out" by their passage through 1029 feet of rock. After the tunnel broke through the PTn, the time lag shortened slightly, and the daily pressure variations became more obvious at Probe #3, indicating a more direct connection had been established between Probe #3 and the atmosphere via the ESF.

Because UE-25 ONC#1 responds to both vertical flow from the surface through the mountain, and horizontal flow from the tunnel, it does not meet the constraints for conventional pulse test analysis. (There may also be horizontal effects from the sides of the mountain.) To determine the effect of tunnel breakthrough on the UE-25 ONC#1 pressures, it would be necessary to remove the effects of the pulsing from the pre-breakthrough pathways, because conventional pulse test analysis techniques are based on one-dimensional, horizontal, cylindrical flow into a well. Inasmuch as the response after breakthrough was similar to the response prior to breakthrough, the inherent inaccuracies involved in trying to remove the pre-breakthrough response from the pressure data would make the pulse test analysis unreliable. Accordingly, the pressure data were reviewed to determine whether other analysis techniques could be applied.

6.2.2.2 REGRESSION ANALYSIS

Regression analysis is a technique for identifying the degree of correlation, if any, between two or more variables (Draper and Smith, 1981). In this case, the pressures for successive probes in UE-25 ONC#1 were compared. Previous well testing and other analyses of Yucca Mountain had indicated high permeabilities are present, so it was expected that there would be a high degree of correlation between the pressures at adjacent probes. This was found to be true.

Analysis graphs were prepared to evaluate the correlation between successive adjacent probes in UE-25 ONC#1 for the period from March 28, 1996 through March 24, 1997. This period was selected for review because it was after known mechanical or operational problems with the probes had been solved, and it constitutes a period of one year of continuous data readings. Each graph contained three plots:

1. A plot of the pressure from each probe versus time. Different pressure scales were used for each probe to show the similarity between the timing of the pressure changes.

2. A linear regression plot of the pressure from the shallower probe on the x-axis, versus the pressure from the deeper probe on the y-axis. If the pressures from the two gauges are perfectly correlated, the data follow a perfect straight line, while if they are poorly correlated, the data are highly scattered.

3. A pressure residual plot showing the residual pressure change in the deeper probe after removing the effect of the correlation to the shallower probe. This plot shows whether there were other changes in the system beside the correlation between the pressures measured at the two probes. Such changes might include for example, seasonal effects, or the effect of continued work on the ESF.

In general, a slope of 1.0 on the correlation plot between pressures means the same pressure changes were observed on both gauges, a slope greater than 1.0 implies the lower gauge saw greater pressure change than the upper gauge, and a slope less than 1.0 implies the lower gauge saw less pressure change than the upper gauge. The correlation coefficient shows how strongly the two readings depend on each other, with a value of 1.0 implying perfect agreement, while a value of 0.0 implies no correlation. The correlation between successive probes accounted for almost all the pressure variability, except between Probe 7 above the water table, and Probe 8 in the saturated section.

The linear regression analysis plots for the correlation between Probes 2 and 3 are shown in Figure 6-2. (Similar analysis graphs were prepared between each pair of successive gauges.) Probe 2 measures the pressure in the Topopah Springs at a depth of 778 feet, while Probe 3 is located in the Topopah Springs unit at a depth of 1029 feet. There was a strong correlation between the pressure at Probe 3 and Probe 2 ($r^2 = 0.9599$). The slope of the best-fit line was 1.0993, which suggests that the pressure changes observed at Probe 3 were *greater* than those at Probe 2. This implies a more direct communication between atmospheric pressure and Probe 3 than Probe 2, which might be indicative of greater horizontal permeability or connecting faults. As well, the correlation was better between Probe 3 and Probe 2 than it was between Probe 1 and Probe 2, suggesting Probe 2 may be receiving more impetus from below than from above. The residuals after accounting for the correlation between the probes were negligible.

The results of the linear regression are summarized below:

Table 6-1: Summary of Regression Results

		Linear Correlation Between Pressures		Residual Correlation with Time	
Upper Probe	Lower Probe	Slope, psi/psi	Correlation Coefficient, r^2	Slope, psi/day	Correlation Coefficient, r^2
0	1	0.8891	0.9272	0.00000	0.0000
1	2	0.4379	0.5328	0.00009	0.1214
2	3	1.0993	0.9599	-0.00001	0.0043
3	4	0.9827	0.9592	0.00002	0.0641
4	5	0.8808	0.8540	-0.00001	0.0087
5	6	1.0732	0.2436	0.00008	0.0104
6	7	0.9352	0.9727	-0.00010	0.0184
7	8	-0.0418	0.0002	-0.00080	0.6843
8	9	1.1020	0.9930	-0.00002	0.0290

The regression analyses between the different gauges indicated Probes 1 through 7 responded to atmospheric pressure changes, which may also have affected to a much lesser degree Probes 8 and 9 below the water table. The gauges showed greater variability from Nov. 1996 through March 1997 than the previous 7 months, which was probably a seasonal effect. There is an indication that Probe 3 has a more direct connection with atmospheric pressure than Probe 2, either through greater horizontal permeability carrying the ESF tunnel effects more efficiently, or through faults. The pressure response at Probe 4 indicated possible changes in the flow paths affecting the gauge around Nov. 1, 1996 and Dec. 20, 1996, or perhaps changes in the gauge sensitivity or measurements around those times. There was a similar indication that Probe 6 may have become better connected to the tunnel around Nov. 1, 1996; if so, the improved connection did not extend to Probes 5 or 7. Alternatively, there may have been a change in the mechanical response of the gauge in Probe 6 at that time. Finally, Probes 8 and 9 below the water table appear to be responding more to other signals than the atmospheric pressure changes. These other factors are presumably associated with

water level changes, which can be much larger in magnitude than atmospheric pressure changes communicated to such depths.

6.2.2.3 FOURIER SERIES ANALYSIS

A Fourier series is a mathematical formula to express an arbitrary periodic function as a series of sinusoidal terms (sines and cosines). The Fourier coefficients (a_n and b_n) for an arbitrary function $f(x)$ with period $2L$ are computed from standard equations (Menzel, 1960) as:

$$f(x) = a_0 + \sum_{n=1}^{\infty} a_n \cos\left(\frac{n\pi x}{L}\right) + b_n \cos\left(\frac{n\pi x}{L}\right), \quad \text{where}$$

$$a_n = \frac{1}{L}\int_0^{2L} f(x)\cos\left(\frac{n\pi x}{L}\right) dx, \quad n = 0 \quad to \quad \infty$$

$$b_n = \frac{1}{L}\int_0^{2L} f(x)\sin\left(\frac{n\pi x}{L}\right) dx, \quad n = 1 \quad to \quad \infty$$

In this case, the measured data were unevenly spaced, and there are some periods with absent data. To adjust for this, it was assumed for the calculation of the Fourier coefficients that pressure was a linear function of time between measured points. A period of 360 days was used. To avoid having the difference between the first and last data points influence the results, a linear trend from the beginning to end was removed prior to computing the Fourier coefficients.

For plotting purposes, the standard forms were converted to an amplitude (c_n) and phase angle (θ_n) as shown below:

$$f(x) = a_0 + \sum_{n=1}^{\infty} c_n \cos\left(\frac{n\pi x}{L} + \vartheta\right), \quad \text{where}$$

$$c_n = \sqrt{a_n^2 + b_n^2}, \quad \vartheta_n = \tan^{-1}\left(-\frac{b_n}{a_n}\right)$$

The Fourier coefficients c_n for the pressure response for Probes 0 through 9 are plotted together in Figure 6-3. From this figure, it was inferred that the coefficients for Probes 0 through 7 all have similar magnitude, with some appearance of anomalous values at 1, ½ and $^1/_3$ day periods (frequencies of 1, 2 and 3 days^{-1}). Probes 8 and 9 have much larger coefficients. The coefficients in all cases are greatest for the low frequencies, and decline rapidly at higher frequencies.

The Fourier coefficients around a period of one day are plotted in Figure 6-4, and around one-half day in Figure 6-5. These figures confirm that there are daily and semi-daily pressure variations, and that they are largest for Probes 0 (atmospheric response), 1 and 6. This may indicate a more direct communication between Probe 6 and the atmosphere either through faults or through the tunnel and subsequent horizontal pressure transients. If the latter explanation is true, it could be an indicator of higher horizontal permeability between the tunnel and Probe 6 than the other probes.

The Fourier coefficients c_n and phase angles θ_n for each probe were computed, and one day and fractional day periods were evident at all probes. The Fourier coefficient and phase angle as a function of frequency were generally similar functions for all probes except Probes 4 and 6, which had much greater scatter in their plots, possibly indicating they were responding to some factors that were different than the other probes.

The Fourier series identifies the components that have a particular frequency, regardless of whether the flow is horizontal, vertical, radial, linear, or through combined flow paths. Unfortunately, the method also may identify false results, either through statistical noise in the data, or through "aliasing", whereby terms with a frequency of one day may falsely appear at frequencies that are multiples of one day. This appears to be the case with the terms at one-half day, one-third day, etc.

6.2.2.4 LOMB SPECTRAL ANALYSIS

Another method for analyzing periodic data is the Fast Fourier transform (or "FFT") technique. The FFT allows a direct computation of the power spectrum, corresponding to the Fourier coefficients, based on a discrete Fourier transform of the data. The FFT methodology requires evenly spaced data. For unevenly spaced data, a variant of the FFT known as the Lomb method is used instead (Press, et al., 1992). In addition to computing the spectral power, the Lomb algorithm also provides a computation of the statistical significance of the results. The use of this technique is best described by reference to one of the figures showing the results. Figure 6-6 shows the computed power spectrum for Probe 0, which measures atmospheric pressure changes. There are numerous frequencies of less than 2.25 $days^{-1}$ (corresponding to periods greater than 0.4 days) that would be expected to arise by chance from noise less than one time in ten thousand. Accordingly, those frequencies are considered statistically significant. The largest factors are those in the upper left corner of the plot, which correspond to longer-term cycles of 30 days period or more. A plot for Probe 3, which measures pressure response in the Topopah Springs unit at a depth of 1029 feet, is shown in Figure 6-7. The Probe 3 response was similar to the Probe 0 (atmospheric) response.

Using similar plots for all probes, it was found that higher frequency data, corresponding to periods of 0.6 days or less, were not significant for Probes 2 through 9. The power spectrum for Probe 6 had a distinctly different shape than the other probes, possibly indicating different flow paths. One possible interpretation for the power spectrum for Probe 6 might be that it is responding to multiple flow paths, with the pressure waves canceling out certain frequencies and reinforcing other frequencies. Only low frequency components, with periods greater than 1.5 days, were significant for Probes 8 and 9, which are below the water table. This implies the daily variations in those two probes are probably not real, but are aliasing effects from other, lower frequency terms.

To provide a better comparison between the power spectrum for the various probes, the results were plotted against each other. In other words, the computed spectral power for each frequency for one probe was plotted against the computed spectral power for another probe at the same frequency. Figure 6-8, for example, is a cross-plot between the Probe 0 and Probe 1 power spectra, indicating these probes respond similarly to each other. (Only the values greater than 10 on this plot are statistically significant.)

6.2.3 RESULTS OF INVESTIGATIONS

The analysis of the UE-25 ONC#1 atmospheric pressure response led to the following conclusions:

Pulse Test Analysis Results

1. Conventional pulse test analysis techniques were not applicable, because there are both horizontal and vertical flow effects.

2. A more detailed, multidimensional analysis (such as the Multimedia Environmental Technology, Inc. model) is necessary for complete analysis of the pressure response.

Regression Analysis

3. Probes 1 through 7 clearly responded to atmospheric pressure changes, which had little or no effect on Probes 8 and 9 below the water table.

4. Greater pressure variability from Nov. 1996 through March 1997 was probably a seasonal effect.

5. Probe 3 has a more direct connection with atmospheric pressure than Probe 2, either through greater horizontal permeability carrying the ESF tunnel effects more efficiently, or through faults.

6. The flow paths affecting Probe 4 apparently changed around Nov. 1, 1996 and Dec. 20, 1996.

7. Probe 6 may have become better connected to the tunnel around Nov. 1, 1996; if so, the improved connection did not extend to Probes 5 or 7.

8. Probes 8 and 9 below the water table responded more to other signals (presumably water level changes) than the atmospheric pressure changes.

Fourier Series Results

9. Daily pressure variations were evident for all probes, and were largest for Probes 0 (atmospheric pressure), 1 and 6.

10. This may indicate the presence of a relatively direct communication between Probe 6 and the atmosphere, either through faults or through the tunnel and subsequent horizontal pressure transients.

11. Probes 4 and 6 have much greater scatter in their plots, possibly indicating they are responding to some factors that are different than the other probes.

Lomb Spectral Analysis

12. The most significant terms were those corresponding to cycles of 30 days or more. Data for periods of 0.6 days or less were not significant for Probes 2 through 9, which implies the high frequency terms were "damped out" by their passage through the mountain.

13. Probe 1 had a response similar to the Probe 0 (atmospheric) response. No other Probe correlated as strongly with Probe 0.

14. Strong correlation was seen between Probes 2 and 3, 2 and 5, and 2 and 7, indicating more similar flow paths or connections for these than the other probes.

15. None of the probes correlated with Probe 4 or 6, implying those two probes are responding to different flow paths.

16. Probe 6 has a power spectrum that is distinctly different from the other probes, possibly indicating different flow paths and pressure interference, with the pressure waves canceling out certain frequencies and reinforcing other frequencies.

17. Probes 8 and 9 below the water table were strongly correlated to each other, and the only significant terms for those probes were the low frequency components (periods > 1.5 days).

6.3 UE-25 ONC#1 VACUUM TESTS

6.3.1 INVESTIGATIVE ACTIVITIES

In June, 1997, vacuum tests were conducted in UE-25 ONC#1 to obtain air samples for laboratory measurements. The pressures recorded during these tests were analyzed using a prolate spheroidal (elliptical) flow analysis technique.

6.3.2 METHODOLOGY

The analysis of the UE-25 ONC#1 vacuum tests was based on the recognition of the presence of wellbore storage, skin, and both cylindrical and spherical flow. When the port connecting to a zone is opened, flow is initially influenced by wellbore storage as air moves from the open region in the annulus between the pipe and the wall of the hole. After the air volume stored in the well is produced, the pressure drop associated with flow from the formation becomes the dominant factor in the pressure response. The flowing pressure drop is caused by two main factors:

- The pressure drop in the region immediately around the well, corresponding to the skin effect.

- The pressure drop further out in the reservoir, which depends on the level of permeability present.

The skin pressure drop and the reservoir pressure drop are often of comparable magnitude, so it is not generally possible to separate their effects from the steady-state response flow alone. Once the zone is shut in, the rate of flow from the formation to the well decreases to a minimal level. During that "late time" period, reservoir effects dominate. Because the flow rate at that time is negligible, so is the skin factor, and it is therefore feasible to separate the effects of the reservoir permeability from the skin effects. The late-time pressure buildup is very small, and care must be taken to minimize wellbore storage, flow rate variability and temperature variability in order to see the spherical flow response.

The test analysis involved constructing spherical flow plots for the buildup (Figure 6-9). After wellbore storage effects die out, the late-time dimensionless response for spherical flow is (Joseph, et al., 1985)

$$P_D = 1 + S - \frac{1}{\sqrt{\pi\, t_D}}$$

Equation 1

where P_D = dimensionless pressure
S = skin factor
t_D = dimensionless time

The dimensionless response is normally given for continuous production. The permeability is one of the proportionality constants in the definition of the dimensionless pressure (and also dimensionless time). For this reason, it is not generally possible to separate the effects of permeability and skin effect from the production portion of the test alone.

For the late-time buildup portion of the test, after wellbore storage effects have died out, the corresponding equation is (Joseph, *et al.*, 1985):

$$P_{F(buildup)} = \left[1 + S - \frac{1}{\sqrt{\pi\,(t_p + \Delta t_p)}}\right] - \left[1 + S - \frac{1}{\sqrt{\pi\,\Delta t_p}}\right] = \frac{1}{\sqrt{\pi\,\Delta t_p}} - \frac{1}{\sqrt{\pi\,(t_p + \Delta t_p)}}$$

Equation 2

Hence, if the buildup pressure is plotted against a function equal to the difference between two reciprocal square roots of time, a straight line should be obtained. The equation of the applicable straight line is:

$$P[psia] = P_i - 2454.26\frac{q[bpd]B[bbl/stb]\mu[cp]}{k^{3/2}[md]}\sqrt{\phi[-]\mu[cp]c[psi^{-1}]}\left(\frac{1}{\sqrt{\Delta t[hr]}} - \frac{1}{\sqrt{t + \Delta t[hr]}}\right)$$

Equation 3

After substituting typical average values for air viscosity (0.018 cp), temperature (60°F), test pressure (13± psia) , and for an assumed porosity of 1%, the permeability is computed from the injection rate (q) and slope of the spherical flow plot (m), as follows:

$$k[md] = \left(33.11\frac{q[Mcfd]}{m[psi\sqrt{hr}]}\right)^{3/2}$$

Equation 4

The intercept of the line is equal to the extrapolated reservoir pressure.

The skin factor is evaluated from the difference between the final injection pressure and the extrapolated reservoir pressure, by neglecting the time dependent term in Equation 1, and converting to conventional units and rearranging as follows:

$$S = \frac{k[md]r_{we}[ft](P_{inj} - P_i)[psia]}{70.627q[bpd]\mu[cp]B[bbl/stb]} - 1$$

Equation 5

The approximate equivalent spherical wellbore radius was estimated using a published formula for prolate spheroidal or elliptical flow (Raghavan and Clark, 1975).

$$r_{we} = \frac{h}{\ln\left[\frac{0.5 + \sqrt{.25 + \left(\frac{r_w}{h}\right)^2 \frac{k_z}{k_h}}}{-0.5 + \sqrt{.25 + \left(\frac{r_w}{h}\right)^2 \frac{k_z}{k_h}}}\right]}$$

Equation 6

6.3.3 RESULTS OF INVESTIGATIONS

Preliminary results indicate the following permeability and skin factors were present:

Table 6-2: UE-25 ONC#1 Vacuum Test Preliminary Results

Test No.	Test Port	Permeability if Skin were Zero, darcies	Corrected Permeability for Non-zero Skin, darcies	Skin Factor
1	5	0.87	5.2	5.0
2	4	0.065	0.31	3.7
3	6	0.33	3.0	8.3
4	N/A	NA	NA	NA
5	2	0.019	0.22	11

The final results will differ slightly (estimated to be within ±20%) from the preliminary results after a more rigorous derivation of the equivalent spherical radius is prepared. These results confirm the presence of high permeability at Yucca Mountain, and are similar to values computed from the SD-12 tests.

The presence of significant skin factors is inferred to occur as a result of incomplete connection to the natural fracture system. Especially in a long test interval such as is present at UE-25 ONC#1, only a few of the existing natural fractures communicate directly to the well. Thus, there is a pressure drop near the well as flow converges into the fractures that do directly communicate with the well, which leads to a so-called skin factor. This topic will be addressed in future work.

6.4 CONCLUSIONS

1. Well UE-25 ONC#1 shows quasi-periodical pressure changes as a result of atmospheric pressure changes. The atmospheric pressure changes show repeated highs and lows corresponding to daily pressure changes, local weather, and seasonal changes.

2. A regression analysis of adjacent gauges showed the existence of preferential pathways for flow in the system. Probes 1 through 7 (above the water table) responded to atmospheric pressure changes, which had little or no effect on Probes 8 and 9 below the water table. Probes #3 and #6 in particular had more direct connection to the atmospheric pressure changes than most of the other probes.

3. Methods for the analysis of sinusoidal functions were applied to evaluate the pressure changes in UE-25 ONC#1. Using Fast Fourier Transform (FFT) methods and the Lomb spectral analysis technique, it was found that the connection between Probe 1 and the surface is mainly the result of vertical flow from the surface. Probe 2 was affected by other factors, probably resulting from horizontal flow through permeable layers below it. Probes 3, 5 and 7 have similar responses to Probe 2. This might indicate fault connection or other conduits for flow between these intervals. Probes 4 and 6 are apparently affected by flow through other pathways. Probe 6 in particular may be seeing the effects of constructive and destructive pressure wave

interference that could be the result of multiple pathways for pressure communication to that probe. Probes 8 and 9 in the saturated zone are largely affected by changes in the water table. These results are shown graphically in Figure 6-10. Although the results are qualitative in that the reservoir properties could not be computed from this approach, preferred flow paths and changes in flow paths were delineated.

4. The pressure data from the vacuum tests were of sufficient quality to allow computation of permeability and skin factor in four horizons. Preliminary analysis results indicated permeability ranging from 0.2 to 5.2 darcies, and skin factors between +3.7 and +11 were present. The presence of significant skin factors is inferred to occur as a result of incomplete connection to the natural fracture system.

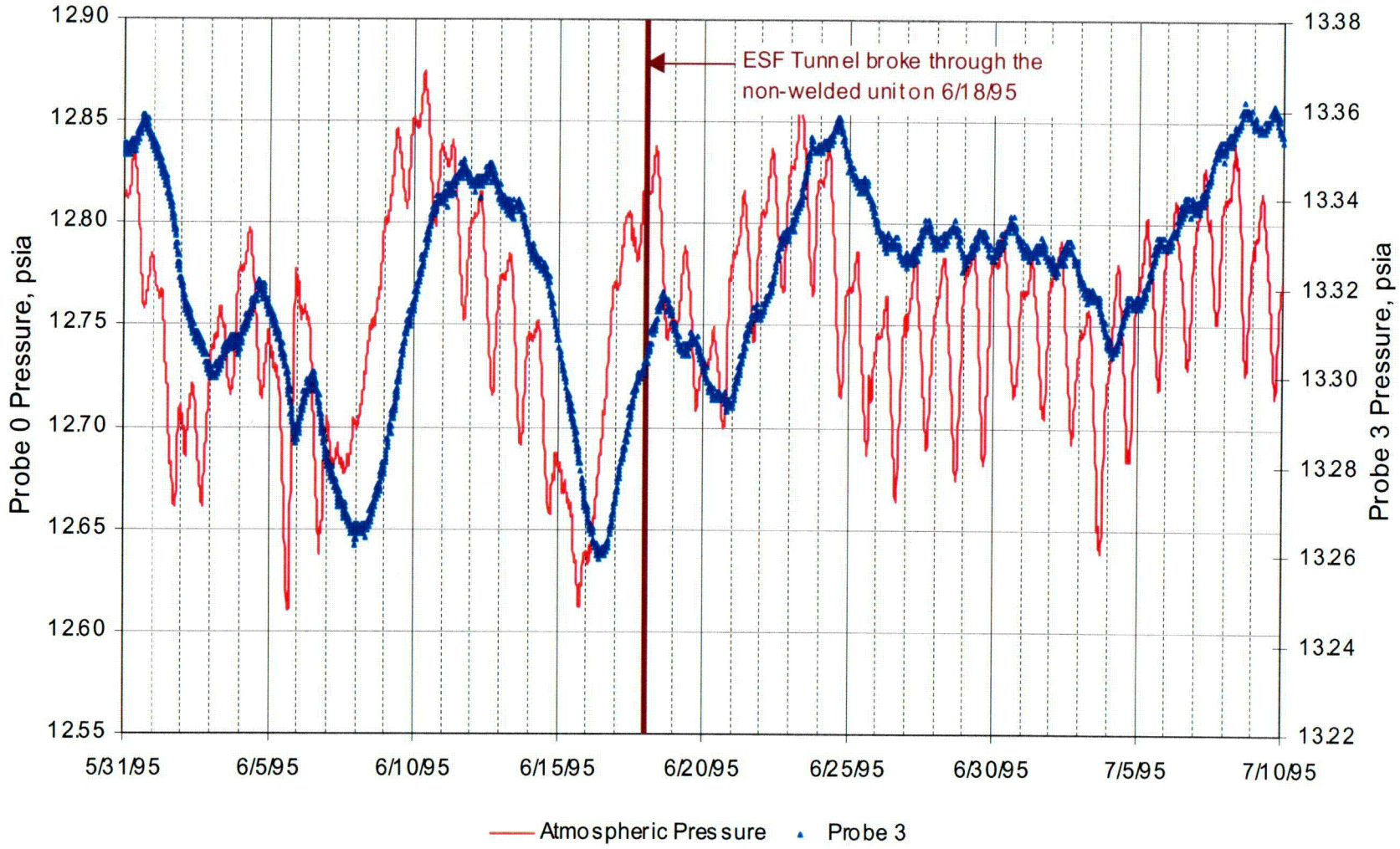

Figure 6-1 Correlation between probes 0 and 3 showing response to ESF breakthrough (ONC#1 pressure response).

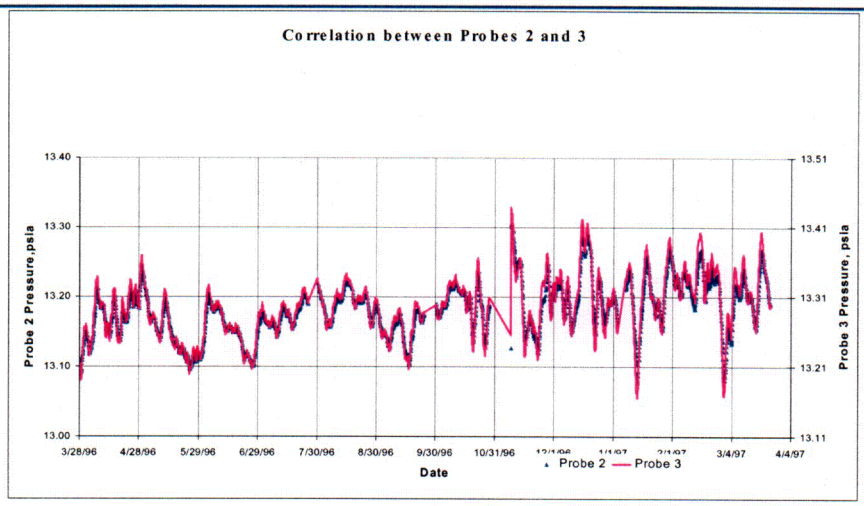

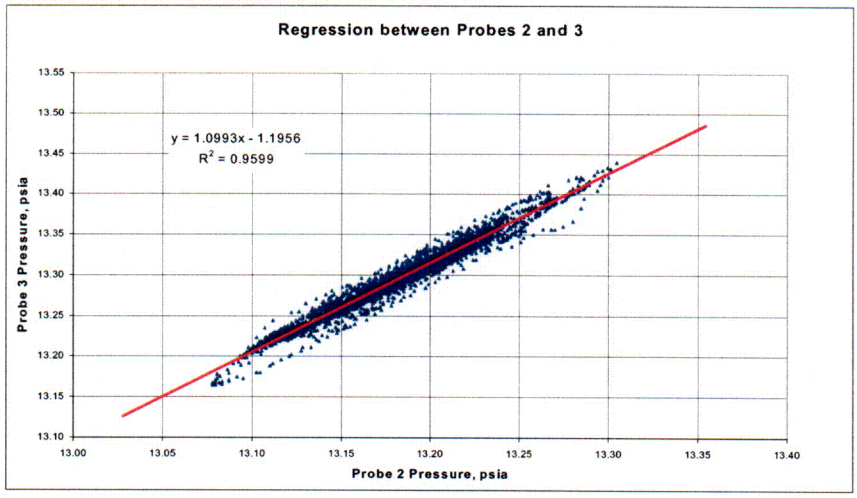

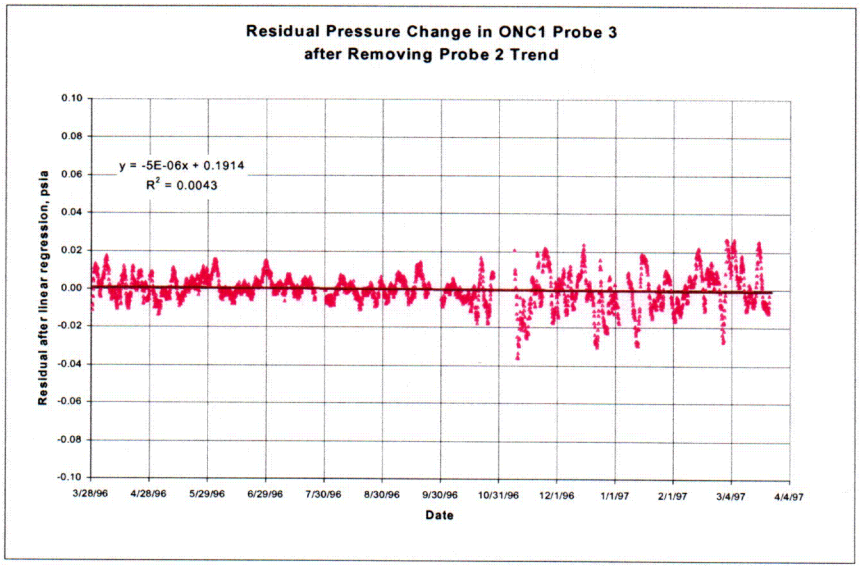

Figure 6-2 Comparison between probes 2 and 3.

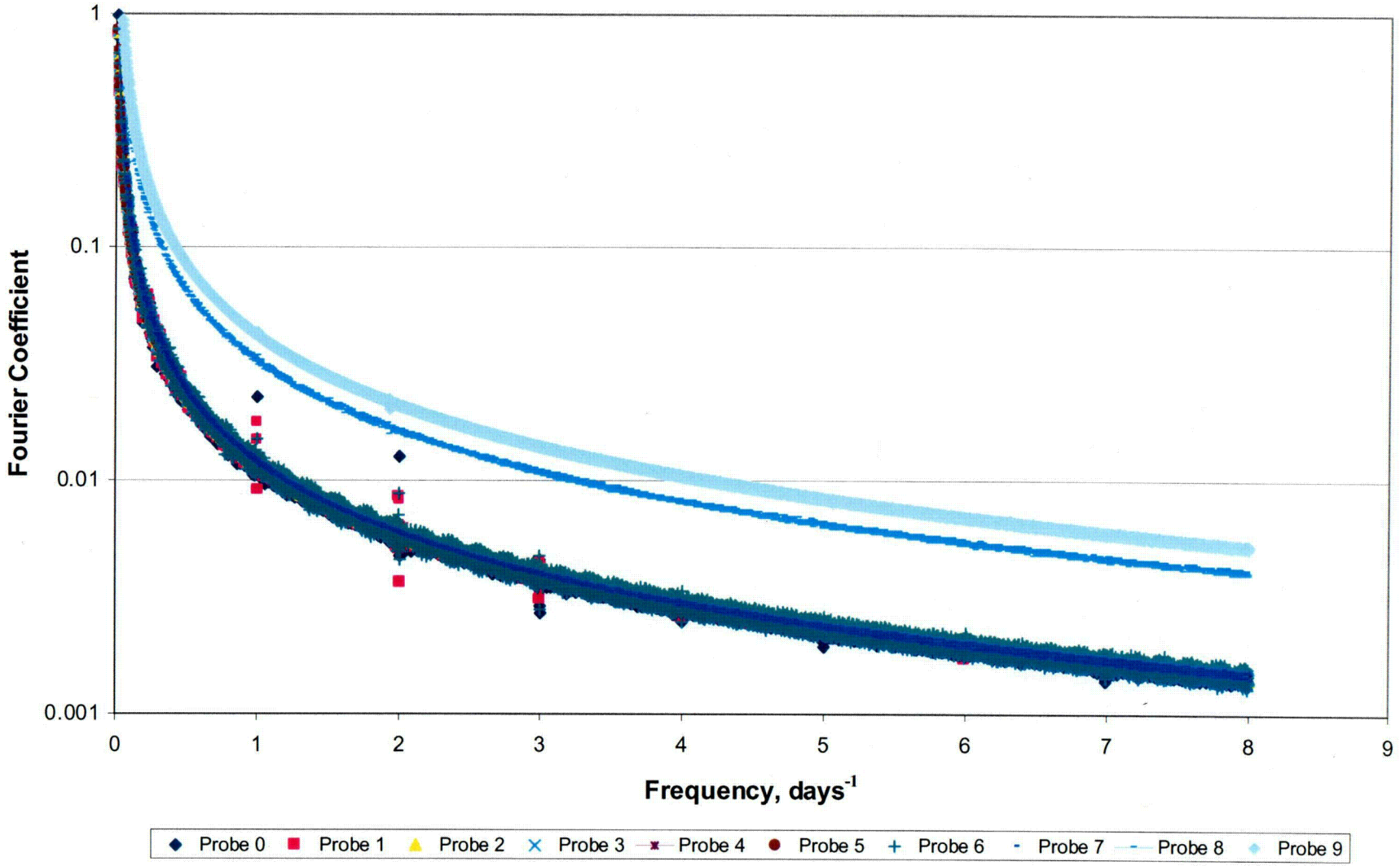

Figure 6-3 Combined frequency response at ONC#1.

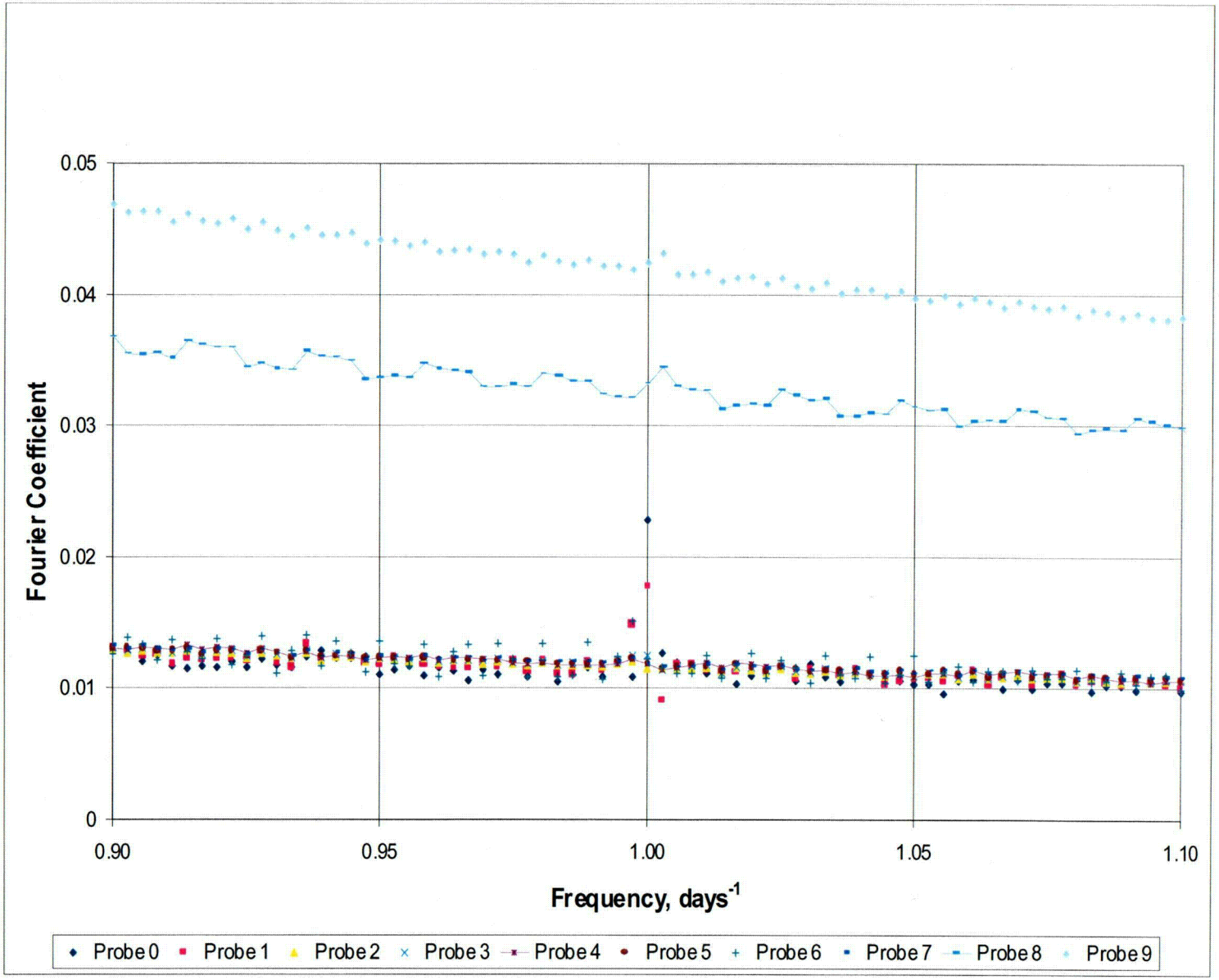

Figure 6-4 **Combined frequency response at ONC#1 around 1 day period.**

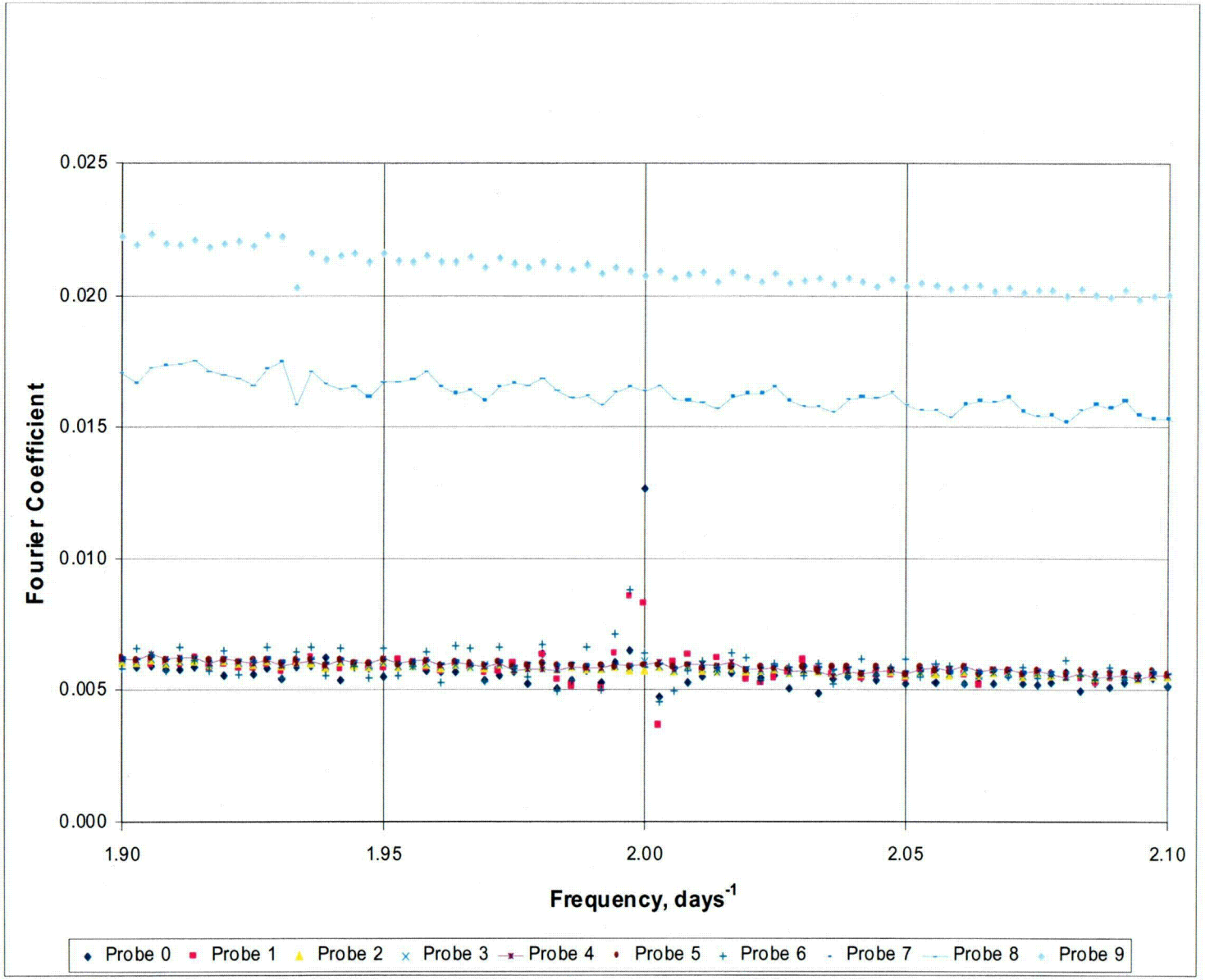

Figure 6-5 **Combined frequency response at ONC#1 around half-day period.**

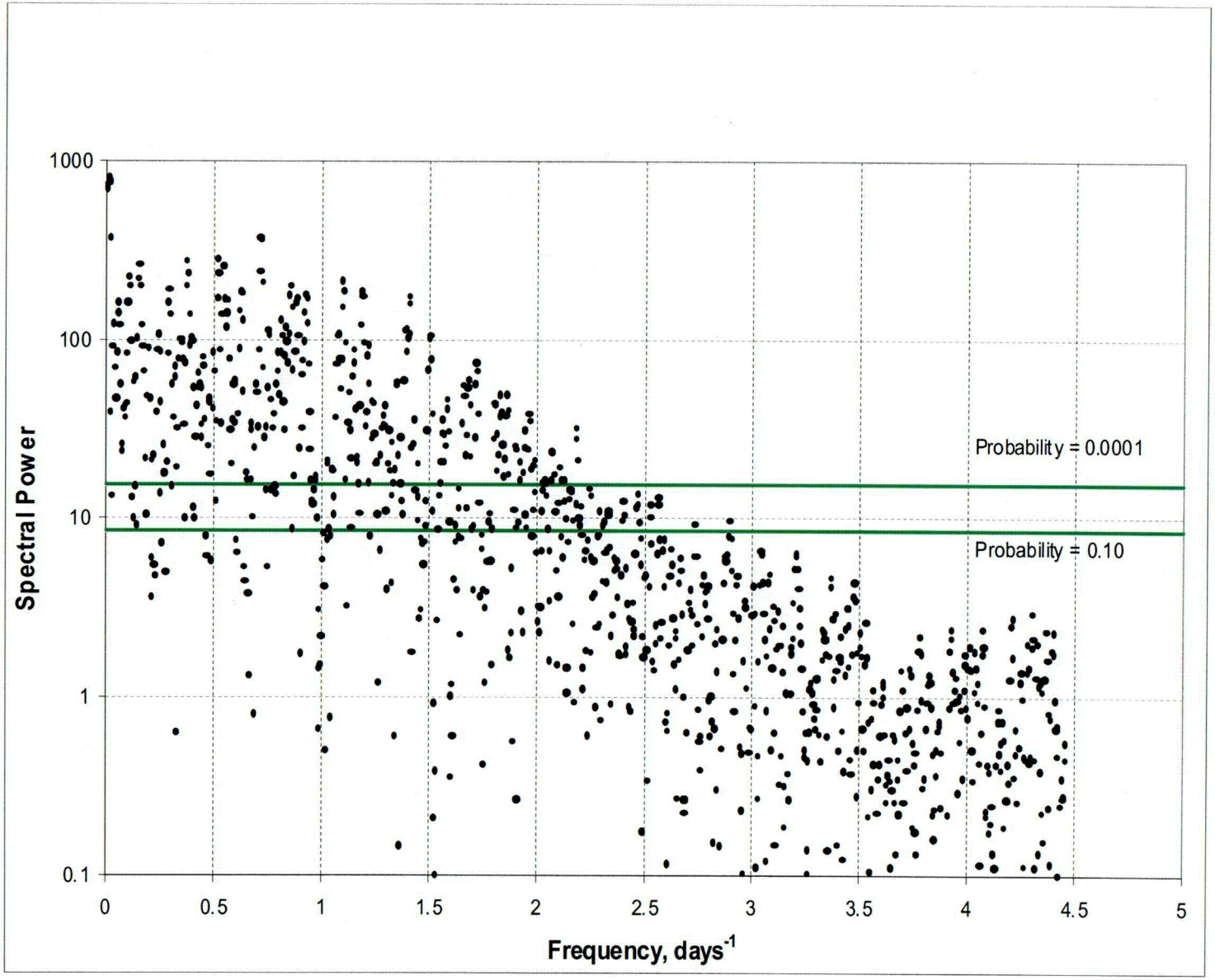

Figure 6-6 Probe 0 response from March 28, 1996 to March 24, 1997 (spectral analysis of ONC#1 pressure).

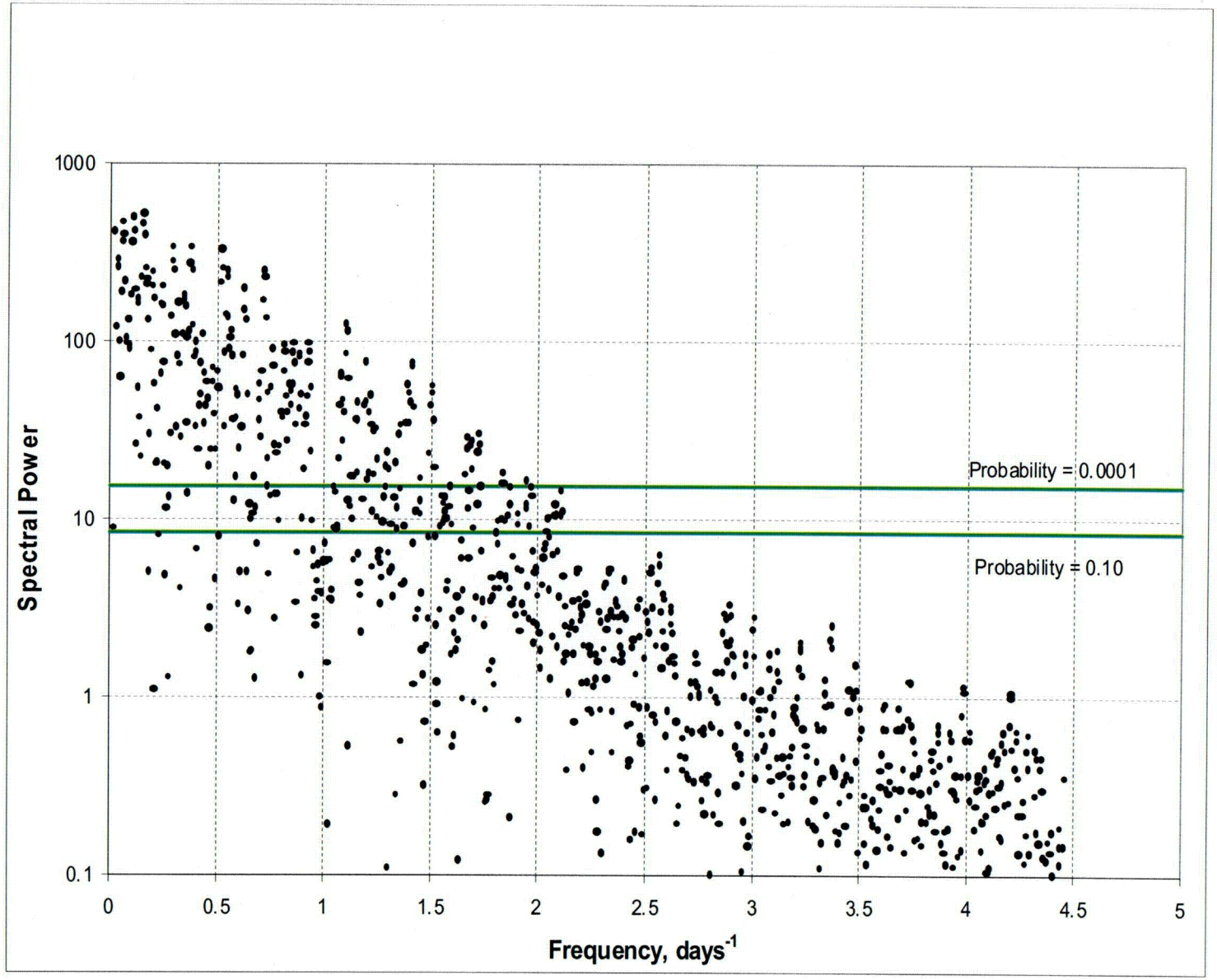

Figure 6-7 **Probe 3 response from March 28, 1996 to March 24, 1997 (spectral analysis of ONC#1 pressure).**

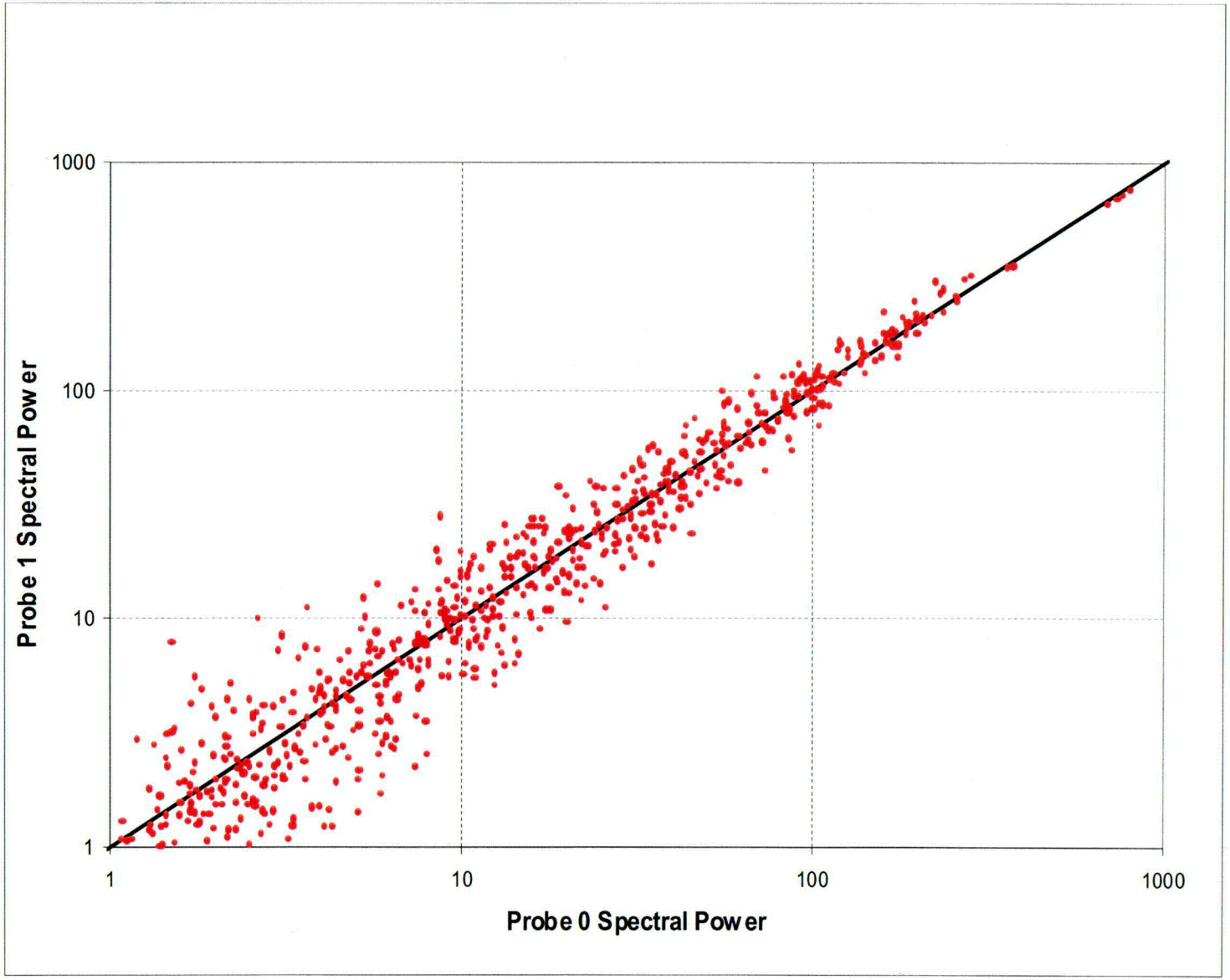

Figure 6-8 Comparison between atmospheric response and probe 1 response from March 28, 1996 to March 24, 1997.

Test Data and Results

Zone Height	180 ft	55 m
Eq. Spherical Wellbore Radius	15.3 ft	4.7 m
Production Rate	0.864 Mcfd	16.1 slpm
Production Flow Time	18 hrs	18 hrs
Total Pressure Change	0.75 psi	5.18 kPa
Permeability for S=0	19 md	1.88E-14 m^2
Permeability (Spherical)	221 md	2.18E-13 m^2
Skin Factor	10.6	10.6

Extrapolated Pressure	13.073 psi	90.14 kPa
Slope of Line	-0.00868 $psi/hr^{1/2}$	-0.05985 $kPa/hr^{1/2}$
Standard Error	0.00057 $psi/hr^{1/2}$	0.00396 $kPa/hr^{1/2}$
Correlation Coefficient, r^2	0.9745	0.9745
Number of Observations	30	30

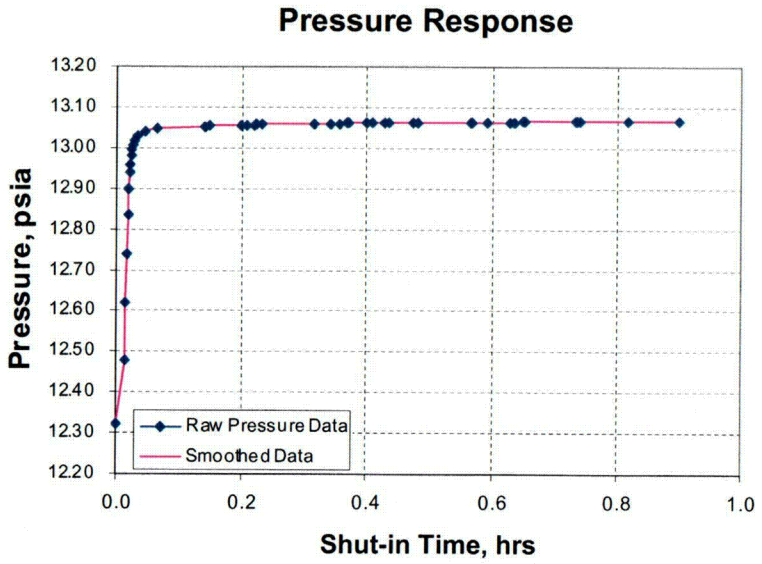

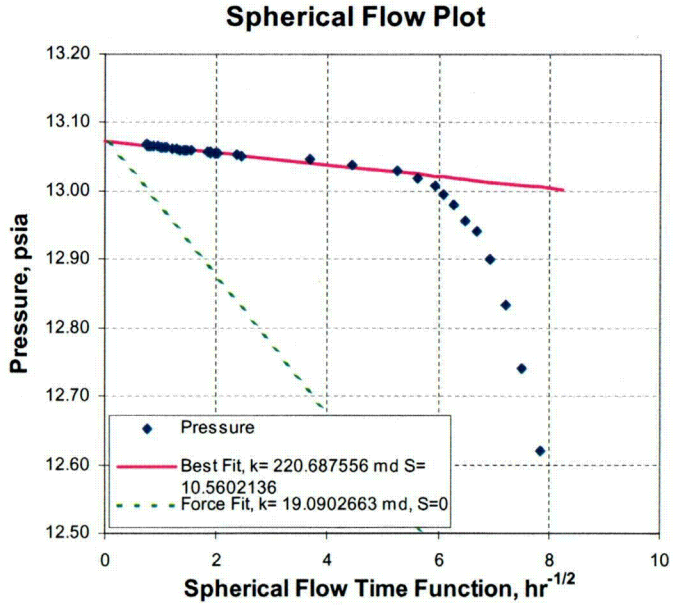

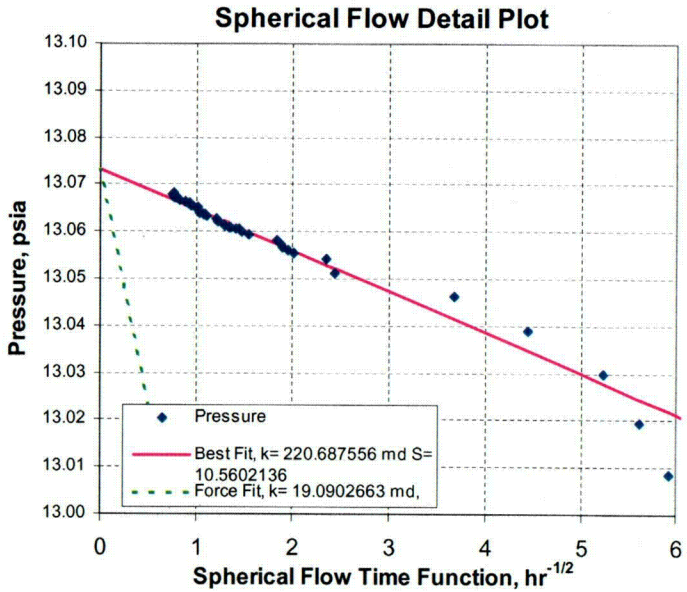

Figure 6-9 ONC#1 vacuum test #5.

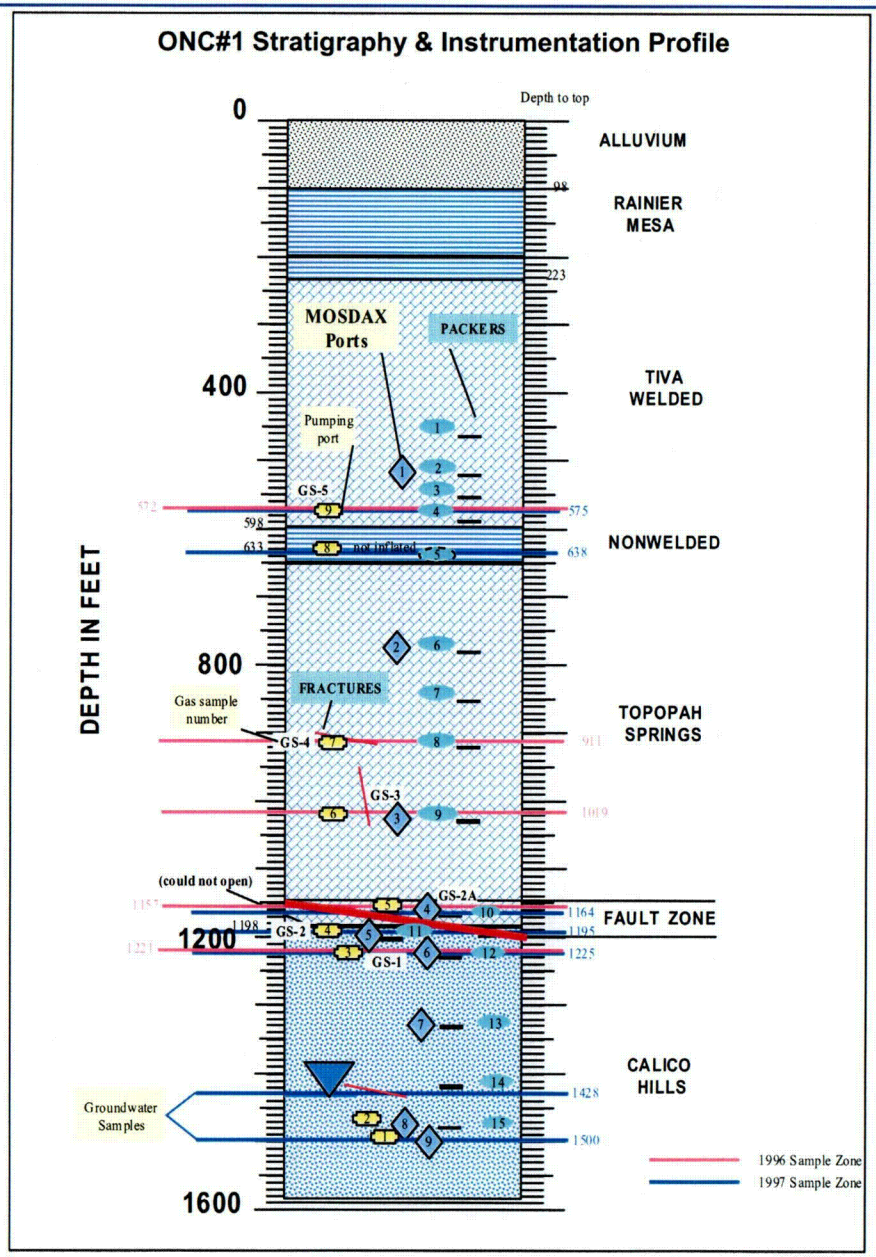

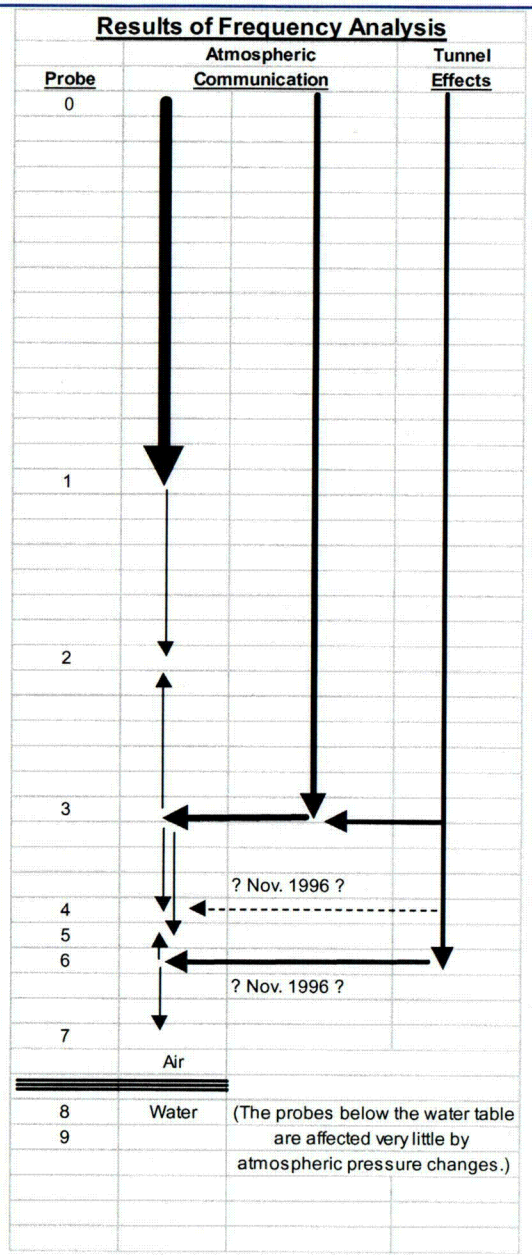

Figure 6-10 ONC#1 well schematic and flow inferences.

C-28